General amplitude of near-threshold hadron scattering for exotic hadrons

Katsuyoshi Sone[*] and Tetsuo Hyodo[†]

Department of Physics, Tokyo Metropolitan University, Hachioji 192-0397, Japan

(Dated: May 15, 2024)

We discuss the general behavior of the scattering amplitude with channel couplings near the two-body threshold. It is known that the Flatté amplitude, which is often used in the analysis of experimental data involving exotic hadrons, has some constraint in the near-threshold energy region. While the M-matrix gives the general expression of the scattering amplitude, it is not smoothly connected to the Flatté amplitude, due to the property of the determinant of the amplitude in channel space. In this paper, based on the effective field theory, we propose new parametrization of the scattering amplitude which gives the general expression near the threshold and has a well-defined limit reproducing the Flatté amplitude. We show that the nonresonant background contribution exists in the general amplitude even in the first order in the momentum. Finally, we quantitatively evaluate the cross sections by changing the strength of the background contribution. We find that the interference with the background term may induce a dip structure of the cross section near the threshold, in addition to the peak and threshold cusp structures.

I. INTRODUCTION

Exotic hadrons are composed of different combinations of quarks from mesons and baryons, and their internal structure still remains unresolved. In recent years, experimental progress has led to the discovery of a wide variety of the exotic hadrons, and various studies have been conducted from both the theoretical and experimental perspectives [1, 2]. Most exotic hadrons are unstable states with finite lifetimes and decay into multiple hadrons, and therefore they are observed as resonance peaks in the hadron scattering. Accumulation of the experimental data reveals that a lot of exotic hadrons appear near the threshold. Furthermore, in actual hadron systems, the channel couplings play an important role by inducing the inelastic scattering in addition to the elastic scattering. As an example, $f_0(980)$ appears near the $K\bar{K}$ threshold and decays into the $\pi\pi$ channel, so we need to consider the coupled-channel scattering of the $\pi\pi$-$K\bar{K}$ system [3].

In the scattering amplitude, the eigenenergy of the resonance state is represented as a pole in the complex energy plane [4, 5]. To express the scattering amplitude with a resonance pole, one utilizes the Breit-Wigner amplitude having a pole at the energy $E = E_R - i\Gamma/2$, where E_R represents the resonance energy and Γ the decay width. Because the Breit-Wigner amplitude with a constant decay width Γ does not include the effect of the threshold, the Breit-Wigner amplitude cannot be applied to the analysis of the resonance state near the threshold. To incorporate the threshold effect into the Breit-Wigner amplitude, the Flatté amplitude [6] has been frequently used for the actual analysis of the various hadron scattering near the threshold [7–20]. In the Flatté amplitude, the opening of the threshold is taken into account by the energy dependence of the decay width Γ.

To study the near-threshold exotic hadrons, it is useful to expand the inverse of the scattering amplitude as the power series of the momentum k of the threshold channel. In the single-channel case, the effective range expansion of the scattering amplitude $f(k)$ reads

$$f(k) = \frac{1}{-\frac{1}{a} + \frac{r}{2}k^2 + \mathcal{O}(k^4) - ik}, \tag{1}$$

where a and r are called the scattering length and effective range, respectively. It is important to determine a and r because the near-threshold dynamics, including the position of the near-threshold pole, is highly constrained by these constants. In the coupled-channel scattering, it is known that the denominator of the Flatté amplitude can also be written in the form of the effective range expansion [21]. This feature allows one to use the Flatté amplitude to determine the scattering length and effective range [22, 23] (see also the discussion in Ref. [24]).

However, a problem of the Flatté amplitude has been pointed out; the number of the independent parameters decreases near the threshold [21]. This fact suggests that some conditions are imposed on the Flatté amplitude near the threshold, lacking the generality of its expression. On the other hand, the general expression of the scattering amplitude consistent with the optical theorem has been constructed, for instance, by using the M-matrix approach [25]. As we will show below, however, the M-matrix type amplitude cannot be directly reduced to the Flatté amplitude due to the implicit assumption in its derivation. To study how the general expression gradually approaches the Flatté amplitude, it is desirable to construct an alternative amplitude, which keeps the generality of the expression but having the smooth connection with the Flatté amplitude.

In this study, we focus on the above-mentioned problems of the near-threshold coupled-channel scattering amplitude and clarify the relation between the general form of the amplitude and the Flatté amplitude. For this purpose, we formulate both the Flatté and M-matrix amplitudes in the framework of the effective field theory.

---

[*] sone-katsuyoshi@ed.tmu.ac.jp

[†] hyodo@tmu.ac.jp

Through the detailed comparison of these amplitudes, we propose a new parametrization of the scattering amplitude that does not lose generality even near the threshold and directly reduces to the Flatté amplitude. This allows us to study how the general behaviors of the scattering length and near-threshold cross sections reduce to those of the Flatté amplitude.

This paper is organized as follows. First, we derive the M-matrix type amplitude (hereafter called the Contact amplitude) and the Flatté amplitude from the effective field theory in Sec. II. We then compare the Flatté amplitude with the Contact amplitude and clarify the imposed conditions by exploring the compatibility between these amplitudes. Next, in Sec. III, we propose a new parametrization of the scattering amplitude (General amplitude) that unifies the Contact amplitude and the Flatté amplitude. Using the General amplitude, we discuss in detail the nature of the scattering amplitude near the threshold. In Sec. IV the behavior of the scattering cross section near the threshold is quantitatively investigated using the General amplitude. A summary is given in the last section. Preliminary results of Sec. III are partly reported in the proceedings of the conference [26].

II. COUPLED-CHANNEL SCATTERING AMPLITUDE

In this section, based on Refs. [27–29], we review the derivation of the Contact amplitude and Flatté amplitude for two-channel scattering from the effective field theory (EFT) in Sec. II A and in Sec. II B, respectively. We discuss the scattering length and effective range in these amplitudes. In Sec. II C, we show that the Contact amplitude does not directly reduce to the Flatté amplitude focusing on the determinant of the scattering amplitude.

A. Contact amplitude

Here we derive the two-channel scattering amplitudes at low energies for systems with contact four-point interaction from effective field theory. The Lagrangian $\mathcal{L}$ in this case is given by [27–29]

$$\mathcal{L}_C = \mathcal{L}_0^C + \mathcal{L}_{int}^C, \tag{2}$$

$$\mathcal{L}_0^C = \psi_1^\dagger \left(i\partial_0 + \frac{\nabla^2}{2m_1} - (m_1 - m_2) \right) \psi_1$$
$$+ \phi_1^\dagger \left(i\partial_0 + \frac{\nabla^2}{2M_1} - (M_1 - M_2) \right) \phi_1$$
$$+ \psi_2^\dagger \left(i\partial_0 + \frac{\nabla^2}{2m_2} \right) \psi_2 + \phi_2^\dagger \left(i\partial_0 + \frac{\nabla^2}{2M_2} \right) \phi_2, \tag{3}$$

$$\mathcal{L}_{int}^C = -c_{ij} \psi_i^\dagger \phi_i^\dagger \phi_j \psi_j + \cdots, \tag{4}$$

where $\mathcal{L}_0^C$ is the free Lagrangian representing the rest energy and non-relativistic kinetic energy of the particles. ψ_i and ϕ_i $(i = 1, 2)$ are the fields corresponding to the two particles in channel i and m_i and M_i $(i = 1, 2)$ represent the masses of the particles in channel i. Since the energy is measured from the threshold of channel 2 in this study, the free Lagrangian $\mathcal{L}_0^C$ includes the contribution of the rest energies of ψ_1 and ϕ_1. $\mathcal{L}_{int}^C$ is the Lagrangian of the four-point interaction that represents the transition between the $\psi_i\phi_i$ and $\psi_j\phi_j$ scattering channels, and c_{ij} is the coupling constant. The higher order terms in the derivative expansion in $\mathcal{L}_{int}^C$ are abbreviated. We consider the low-energy scattering, where the contact interaction in Eq. (4) dominates and the higher-order terms are assumed to be negligible.

The Feynman rules obtained from the Lagrangian $\mathcal{L}_C$ give the vertex V_C as

$$V_C = \begin{pmatrix} c_{11} & c_{12} \\ c_{12} & c_{22} \end{pmatrix}, \tag{5}$$

with the bare parameters c_{11}, c_{12}, and c_{22}. The (i, j) components of V_C describe the direct transition process from the scattering channel j to i. Since we are interested in the two-body scattering, we consider the four-point function T_{ij} by adding up all possible diagrams for the two-body to two-body process obtained from the Feynman rules. In the present case, the four-point function is given only by the diagrams obtained from the Lippmann-Schwinger equation, in which V_C is regarded as a potential. The resulting four-point function, the T-matrix of this scattering, depends only on the total energy E in the center-of-mass system:

$$[T(E)]^{-1} = [V_C]^{-1} - G^\Lambda(E), \tag{6}$$

where

$$G^\Lambda(E) = \begin{pmatrix} G_1^\Lambda(E) & 0 \\ 0 & G_2^\Lambda(E) \end{pmatrix}$$
$$= \begin{pmatrix} -\frac{\mu_1 \Lambda}{\pi^2} - \frac{\mu_1}{2\pi} ip & 0 \\ 0 & -\frac{\mu_2 \Lambda}{\pi^2} - \frac{\mu_2}{2\pi} ik \end{pmatrix}, \tag{7}$$

$$G_i^\Lambda(E) = \int \frac{d\boldsymbol{q}}{(2\pi)^3} \frac{1}{E + \Delta\delta_{i1} - \boldsymbol{q}^2/(2\mu_i) + i0^+}, \tag{8}$$

where $\Delta = (M_2 + m_2) - (M_1 + m_1)$ is the threshold energy difference, $\mu_i = M_i m_i/(M_i + m_i)$ the reduced mass in channel i, and $p = \sqrt{2\mu_1(E + \Delta)}, k = \sqrt{2\mu_2 E}$ the relative momenta of channels 1 and 2, respectively. Since the potential V_C is a contact interaction, we have introduced the cutoff Λ, the upper limit of the momentum integral to regularize $G^\Lambda(E)$, by keeping the leading contribution in the $\Lambda \to \infty$ limit in Eq. (7).

Substituting V_C into Eq. (6), we obtain

$$[T(E)]^{-1}$$
$$= \begin{pmatrix} \frac{c_{22}}{c_{11}c_{22} - c_{12}^2} + \frac{\mu_1 \Lambda}{\pi^2} + \frac{\mu_1}{2\pi} ip & -\frac{c_{12}}{c_{11}c_{22} - c_{12}^2} \\ -\frac{c_{12}}{c_{11}c_{22} - c_{12}^2} & \frac{c_{11}}{c_{11}c_{22} - c_{12}^2} + \frac{\mu_2 \Lambda}{\pi^2} + \frac{\mu_2}{2\pi} ik \end{pmatrix}. \tag{9}$$

To perform the renormalization, we define the physical quantities a_{11}, a_{12}, and a_{22} so that the T-matrix takes the form

$$[T(E)]^{-1} = \begin{pmatrix} \frac{\mu_1}{2\pi}\frac{1}{a_{11}} + \frac{\mu_1}{2\pi}ip & -\frac{\sqrt{\mu_1\mu_2}}{2\pi}\frac{1}{a_{12}} \\ -\frac{\sqrt{\mu_1\mu_2}}{2\pi}\frac{1}{a_{12}} & \frac{\mu_2}{2\pi}\frac{1}{a_{22}} + \frac{\mu_2}{2\pi}ik \end{pmatrix}. \quad (10)$$

Comparing Eq. (10) with Eq. (9), we introduce the cutoff Λ dependence in the bare parameters c_{11}, c_{12}, and c_{22} so that a_{11}, a_{12}, and a_{22} are cutoff-independent:

$$\frac{c_{22}(\Lambda)}{c_{11}(\Lambda)c_{22}(\Lambda) - c_{12}^2(\Lambda)} + \frac{\mu_1\Lambda}{\pi^2} = \frac{\mu_1}{2\pi}\frac{1}{a_{11}}, \quad (11)$$

$$\frac{c_{11}(\Lambda)}{c_{11}(\Lambda)c_{22}(\Lambda) - c_{12}^2(\Lambda)} + \frac{\mu_2\Lambda}{\pi^2} = \frac{\mu_2}{2\pi}\frac{1}{a_{22}}, \quad (12)$$

$$\frac{c_{12}(\Lambda)}{c_{11}(\Lambda)c_{22}(\Lambda) - c_{12}^2(\Lambda)} = \frac{\sqrt{\mu_1\mu_2}}{2\pi}\frac{1}{a_{12}}. \quad (13)$$

Taking the $\Lambda \to \infty$ limit with the physical quantities a_{11}, a_{12}, and a_{22} kept finite, the inverse matrix of the scattering amplitude is given by

$$[f^{\mathrm{C}}(E)]^{-1} = \begin{pmatrix} -\frac{1}{a_{11}} - ip & \frac{1}{a_{12}} \\ \frac{1}{a_{12}} & -\frac{1}{a_{22}} - ik \end{pmatrix}, \quad (14)$$

where the relation between the T-matrix and scattering amplitude $f_{ij} = -\sqrt{\mu_i\mu_j}T_{ij}/(2\pi)$ is used. From Eq. (14), we obtain the scattering amplitude

$$f^{\mathrm{C}}(E) = \frac{1}{\frac{1}{a_{12}^2} - \left(\frac{1}{a_{11}} + ip\right)\left(\frac{1}{a_{22}} + ik\right)}$$
$$\times \begin{pmatrix} \frac{1}{a_{22}} + ik & \frac{1}{a_{12}} \\ \frac{1}{a_{12}} & \frac{1}{a_{11}} + ip \end{pmatrix}. \quad (15)$$

Hereafter, we call this amplitude $f^{\mathrm{C}}(E)$ the Contact amplitude.

It is instructive to discuss the relation between the Contact amplitude and the two-channel M-matrix type scattering amplitude derived from the optical theorem. The general form of the inverse of the two-channel scattering amplitude is given as

$$[f(E)]^{-1} = \begin{pmatrix} M_{11}(E) - ip & M_{12}(E) \\ M_{12}(E) & M_{22}(E) - ik \end{pmatrix}, \quad (16)$$

using the M-matrix $M_{ij}(E)$, which is a function of the energy [25]. In Eq. (16), by setting $M_{ij}(E)$ as a constant $M_{ij} = 1/a_{ij}$, we recover the Contact amplitude (14). In other words, it can be seen that the Contact amplitude $f^{\mathrm{C}}(E)$ in Eq. (15) is a special case of the M-matrix type scattering amplitude. This ensures that $f^{\mathrm{C}}(E)$ is a general low-energy scattering amplitude consistent with the optical theorem near the threshold where the higher-order terms in energy E can be neglected. From Eq. (15), we find that the general form of the two-channel scattering amplitude is characterized by three parameters a_{11}, a_{12}, and a_{22} near the threshold. In general, by imposing the time-reversal symmetry on the M-matrix representation, the off-diagonal components of the M-matrix

becomes $M_{ij} = M_{ji}$, so the N channel scattering amplitude has $N(N+1)/2$ independent parameters near the threshold (see Appendix A).

We now discuss the scattering length and effective range at the threshold of channel 2 (higher energy threshold) using the Constant amplitude in Eq. (15). Expanding the denominator of the (2,2) component of the scattering amplitude $f_{22}^{\mathrm{C}}(E)$ in terms of the momentum k, we obtain

$$f_{22}^{\mathrm{C}}(E) = \left[\frac{1}{a_{12}^2\left(\frac{1}{a_{11}} + ip_0\right)} - \frac{1}{a_{22}} \right.$$
$$\left. - \frac{i}{2a_{12}^2\left(\frac{1}{a_{11}} + ip_0\right)^2 p_0}k^2 - ik + \mathcal{O}(k^4) \right]^{-1}, \quad (17)$$

where $p_0 = \sqrt{2\mu_1\Delta}$ represents the momentum of channel 1 at the threshold of channel 2. The denominator of $f_{22}^{\mathrm{C}}(E)$ is composed only of the even powers in k, except for the term $-ik$. Therefore, $f_{22}^{\mathrm{C}}(E)$ can be written in the form of the effective range expansion in k, the momentum of channel 2. As in the case of the single channel scattering (1), we define the scattering length a_{C} from the constant term and the effective range r_{C} from the coefficient of the k^2 term in the denominator of $f_{22}^{\mathrm{C}}(E)$ in Eq. (17). The scattering length a_{C} is given by

$$a_{\mathrm{C}} = \frac{a_{12}^2 a_{22}(1 + ip_0 a_{11})}{a_{12}^2(1 + ip_0 a_{11}) - a_{11}a_{22}}. \quad (18)$$

For later discussion, we decompose a_{C} into the real and imaginary parts:

$$a_{\mathrm{C}} = \frac{a_{12}^4 a_{22}(1 + p_0^2 a_{11}^2) - a_{11}a_{12}^2 a_{22}^2}{(a_{12}^2 - a_{11}a_{22})^2 + p_0^2 a_{11}^2 a_{12}^4}$$
$$- i\frac{p_0 a_{11}^2 a_{12}^2 a_{22}^2}{(a_{12}^2 - a_{11}a_{22})^2 + p_0^2 a_{11}^2 a_{12}^4}. \quad (19)$$

This expression confirms the relation $\mathrm{Im}(a_{\mathrm{C}}) < 0$ required by the optical theorem. Similarly, the effective range r_{C} is obtained as

$$r_{\mathrm{C}} = -\frac{i}{p_0}\left\{\frac{a_{11}}{a_{12}(1 + ip_0 a_{11})}\right\}^2. \quad (20)$$

Note that both a_{C} and r_{C} are in general complex, reflecting the effect of the decay into channel 1. We also expand the denominator of the (1,1) component of the scattering amplitude $f_{11}^{\mathrm{C}}(E)$ (lower energy channel) in terms of k

$$f_{11}^{\mathrm{C}}(E) = \frac{a_{12}^2}{a_{22}^2}\left[\frac{1}{a_{22}} - \frac{a_{12}^2}{a_{11}a_{22}^2} - i\frac{a_{12}^2}{a_{22}^2}p_0 \right.$$
$$\left. - \left(a_{22} + i\frac{a_{12}^2}{2a_{22}^2 p_0}\right)k^2 - ik + \mathcal{O}(k^3) \right]^{-1}. \quad (21)$$

In contrast to $f_{22}^{\mathrm{C}}(E)$, the denominator of $f_{11}^{\mathrm{C}}(E)$ contains the terms of k^3 or more odd powers. Therefore, $f_{11}^{\mathrm{C}}(E)$

cannot be written in the form of the effective range expansion in k, and the scattering length and effective range should be defined not in $f_{11}^{\mathrm{C}}(E)$ but in $f_{22}^{\mathrm{C}}(E)$.

We comment on the higher order corrections to the effective range of the Contact amplitude r_{C} in Eq. (20), which is written only by the parameters a_{11}, a_{12}, and a_{22}. Considering the higher order terms of the interaction Lagrangian in the derivative expansion, one can enlarge the applicable energy region of the EFT. The inclusion of the next-to-leading order terms gives the scattering amplitude

$$[f^{\mathrm{C}}(E)]^{-1} \simeq \begin{pmatrix} -\frac{1}{a_{11}} + a_{11}^{(2)}k^2 - ip & \frac{1}{a_{12}} + a_{12}^{(2)}k^2 \\ \frac{1}{a_{12}} + a_{12}^{(2)}k^2 & -\frac{1}{a_{22}} + a_{22}^{(2)}k^2 - ik \end{pmatrix},$$
(22)

where $a_{11}^{(2)}, a_{12}^{(2)}$ and $a_{22}^{(2)}$ are the coefficients of the k^2 terms. The scattering length a_{C} determined by $f_{22}^{\mathrm{C}}(E)$ in Eq. (22) remains unchanged from the expression in Eq. (18), i.e., a_{C} does not suffer from the higher order corrections. In contrast, the effective range r_{C} contains the higher order corrections with $a_{11}^{(2)}, a_{12}^{(2)}$ and $a_{22}^{(2)}$. Thus, the expression of r_{C} in Eq. (20) is valid only in the leading order EFT, and the value can be modified by including the higher order corrections.

B. Flatté amplitude

In this section, we first show the derivation of the Flatté amplitude in the EFT. The Lagrangian that gives the Flatté amplitude is [30]

$$\mathcal{L}_{\mathrm{F}} = \mathcal{L}_0^{\mathrm{F}} + \mathcal{L}_{\mathrm{int}}^{\mathrm{F}},$$
(23)

$$\mathcal{L}_0^{\mathrm{F}} = \psi_1^\dagger \left(i\partial_0 + \frac{\nabla^2}{2m_1} - (m_1 - m_2) \right) \psi_1$$
$$+ \phi_1^\dagger \left(i\partial_0 + \frac{\nabla^2}{2M_1} - (M_1 - M_2) \right) \phi_1$$
$$+ \psi_2^\dagger \left(i\partial_0 + \frac{\nabla^2}{2m_2} \right) \psi_2 + \phi_2^\dagger \left(i\partial_0 + \frac{\nabla^2}{2M_2} \right) \phi_2$$
$$+ \Psi^\dagger \left(i\partial_0 + \frac{\nabla^2}{2M} - \nu \right) \Psi,$$
(24)

$$\mathcal{L}_{\mathrm{int}}^{\mathrm{F}} = \hat{g}_i \left(\psi_i^\dagger \phi_i^\dagger \Psi + \Psi^\dagger \phi_i \psi_i \right),$$
(25)

where $\mathcal{L}_0^{\mathrm{F}}$ is the free Lagrangian and $\mathcal{L}_{\mathrm{int}}^{\mathrm{F}}$ is the interaction Lagrangian. In addition to the ψ_i and ϕ_i fields, we introduce the bare field Ψ with mass M. The parameter $\nu = M - (m_2 + M_2)$ represents the bare energy measured from the threshold of channel 2. The parameter $\hat{g}_i$ stands for the coupling constant between the scattering state of channel i and the bare field.

From the Lagrangian $\mathcal{L}_{\mathrm{F}}$, the coupled-channel potential $V_{\mathrm{F}}(E)$ for the two-body to two-body process is given

by

$$V_{\mathrm{F}}(E) = \frac{1}{E - \nu} \begin{pmatrix} \hat{g}_1^2 & \hat{g}_1\hat{g}_2 \\ \hat{g}_1\hat{g}_2 & \hat{g}_2^2 \end{pmatrix},$$
(26)

using the bare parameters $\nu, \hat{g}_1$, and $\hat{g}_2$. The potential $V_{\mathrm{F}}(E)$ describes the transition between the scattering states through the s-channel exchange of the bare field Ψ. It follows from the expression (26) that $\det[V_{\mathrm{F}}(E)] = 0$, and therefore $V_{\mathrm{F}}(E)$ does not have the inverse matrix. Hence, V_{F} cannot be directly substituted into the expression (6) and we use an equivalent equation without V^{-1}:

$$T(E) = [\hat{1} - V(E)G^\Lambda(E)]^{-1}V(E).$$
(27)

Substituting $V_{\mathrm{F}}(E)$ into Eq. (27), we obtain the T-matrix

$$T(E) = \left[E - \nu + \hat{g}_1^2 \left(\frac{\mu_1\Lambda}{\pi^2} + \frac{\mu_1}{2\pi}ip \right) \right. $$
$$\left. + \hat{g}_2^2 \left(\frac{\mu_2\Lambda}{\pi^2} + \frac{\mu_2}{2\pi}ik \right) \right]^{-1} \begin{pmatrix} \hat{g}_1^2 & \hat{g}_1\hat{g}_2 \\ \hat{g}_1\hat{g}_2 & \hat{g}_2^2 \end{pmatrix}.$$
(28)

To perform the renormalization, we define the physical quantities E_{BW}, g_1, and g_2 so that the T-matrix takes the form

$$T(E) = \frac{1}{2E - 2E_{\mathrm{BW}} + ig_1^2 p + ig_2^2 k}$$
$$\times \begin{pmatrix} \frac{2\pi}{\mu_1}g_1^2 & \frac{2\pi}{\sqrt{\mu_1\mu_2}}g_1g_2 \\ \frac{2\pi}{\sqrt{\mu_1\mu_2}}g_1g_2 & \frac{2\pi}{\mu_2}g_2^2 \end{pmatrix}.$$
(29)

Comparing Eq. (28) with Eq. (29), we introduce the cutoff Λ dependence in the bare parameters $\nu, \hat{g}_1$, and $\hat{g}_2$ so that E_{BW}, g_1, and g_2 are cuttoff-independent:

$$\nu(\Lambda) - g_1^2 \frac{\Lambda}{\pi} - g_2^2 \frac{\Lambda}{\pi} = E_{\mathrm{BW}},$$
(30)

$$\hat{g}_1(\Lambda) = \sqrt{\frac{\pi}{\mu_1}}g_1,$$
(31)

$$\hat{g}_2(\Lambda) = \sqrt{\frac{\pi}{\mu_2}}g_2.$$
(32)

Note that there is no Λ-dependence in the coupling constants $\hat{g}_1$ and $\hat{g}_2$. Taking the $\Lambda \to \infty$ limit with the physical quantity E_{BW} kept finite, the Flatté scattering amplitude is obtained as

$$f^{\mathrm{F}}(E) = \frac{1}{2E_{\mathrm{BW}} - 2E - ig_1^2 p - ig_2^2 k}$$
$$\times \begin{pmatrix} g_1^2 & g_1g_2 \\ g_1g_2 & g_2^2 \end{pmatrix},$$
(33)

It is clear in Eq. (33) that the energy dependence of the Flatté amplitude is common to all the coupled-channel components. The expansion of the denominator of each component in powers of k is given by

$$f_{ij}^{\mathrm{F}}(E) \propto \frac{1}{\frac{2E_{\mathrm{BW}} - ig_1^2 p_0}{g_2^2} - \left(\frac{1}{\mu_2 g_2^2} + i\frac{g_1^2}{2p_0 g_2^2} \right) k^2 + \mathcal{O}(k^4) - ik}.$$
(34)

In this way, all the components of the Flatté amplitude are compatible with the effective range expansion, in contrast to the Contact amplitude. We thus determine the scattering length (a_{F}) and effective range (r_{F}) of the Flatté amplitude as

$$a_{\mathrm{F}} = \frac{g_2^2}{i g_1^2 p_0 - 2 E_{\mathrm{BW}}}, \tag{35}$$

$$r_{\mathrm{F}} = -\frac{2}{\mu_2 g_2^2} - i \frac{g_1^2}{p_0 g_2^2}. \tag{36}$$

The imaginary part of the effective range in Eq. (36) stems from the expansion of p (momentum of channel 1) in terms of k. When the threshold energy difference Δ is large, the momentum p can be approximated by its threshold value p_0, as was done in Ref. [21]. In this case, the imaginary part does not appear and r_{F} is obtained as a negative real value.

It was pointed out that the number of parameters in the Flatté amplitude decreases near the threshold, due to the scaling behavior [21]. From Eq. (33), one finds that the Flatté amplitude generally has three parameters, E_{BW}, g_1, and g_2. To consider the scattering in the low-energy region near the threshold of channel 2, we keep the terms up to linear order in k in the denominator, and $f^{\mathrm{F}}(E)$ takes the form

$$f^{\mathrm{F}}(E) \simeq \frac{1}{\frac{\alpha}{R} p_0 - i \frac{1}{R} p_0 - ik} \begin{pmatrix} \frac{1}{R} & \sqrt{\frac{1}{R}} \\ \sqrt{\frac{1}{R}} & 1 \end{pmatrix}, \tag{37}$$

where we define the parameters R and α as

$$\frac{g_2^2}{g_1^2} = R, \qquad \frac{2 E_{\mathrm{BW}}}{g_1^2 p_0} = \alpha, \tag{38}$$

This gives the approximation of the Flatté amplitude up to the first order of k. In the following, for simplicity, the approximated amplitude in Eq. (37) is also referred to as the Flatté amplitude. Equation (37) shows that the Flatté amplitude can be expressed only by two parameters R and α near the threshold. In other words, three parameters of the Flatté amplitude are reduced to two near threshold [21]. As mentioned in Sec. II A, the near-threshold two-channel scattering amplitude generally has three independent parameters. This indicates that some constraint is imposed on the Flatté amplitude near the threshold.

C. Comparison of two amplitudes

We have seen that there is some constraint in the Flatté amplitude which reduces the number of independent parameters. To clarify this constraint, we focus on the determinant of the scattering amplitude matrix. From the separable form of the residue in Eq. (33), one finds that the rank of the matrix $f^{\mathrm{F}}(E)$ is one, and therefore its determinant vanishes:

$$\det\left[f^{\mathrm{F}}(E)\right] = 0. \tag{39}$$

This is caused by the same property of the potential $V_{\mathrm{F}}(E)$ we mentioned in Eq. (26):

$$\det\left[V_{\mathrm{F}}(E)\right] = 0. \tag{40}$$

As seen in Eq. (27), $\det\left[f(E)\right] = 0$ holds for the potential satisfying $\det\left[V(E)\right] = 0$. Physically speaking, the vanishing of the determinant is due to the pole term nature of $V_{\mathrm{F}}(E)$ and $f^{\mathrm{F}}(E)$. It is known that the residue matrix of the pole term in the coupled-channel scattering should be rank one [4], and both $V_{\mathrm{F}}(E)$ and $f^{\mathrm{F}}(E)$ are given by a single pole term without any background scattering contribution. The condition (39) can be related to the constraint imposed on the Flatté amplitude near the threshold.

The Contact amplitude $f^{\mathrm{C}}(E)$ is considered as a general form of the two-channel scattering amplitude near the threshold. It is therefore expected that $f^{\mathrm{C}}(E)$ reduces to the Flatté amplitude near the threshold by imposing the condition $\det\left[f^{\mathrm{C}}(E)\right] = 0$. From Eq. (15), the determinant of $f^{\mathrm{C}}(E)$ is given by

$$\det\left[f^{\mathrm{C}}(E)\right] = -\frac{1}{\frac{1}{a_{12}^2} - \left(\frac{1}{a_{11}} + ip\right)\left(\frac{1}{a_{22}} + ik\right)}, \tag{41}$$

which is nonzero for finite a_{11}, a_{12}, and a_{22}. The condition $\det\left[f^{\mathrm{C}}(E)\right] = 0$ is achieved by letting at least one of a_{11}, a_{12}, and a_{22} be zero. When we take the limit $a_{22} \to 0$ with $a_{12} \neq 0$ and $a_{11} \neq 0$, the Contact amplitude reduces to

$$f^{\mathrm{C}}(E) = \frac{1}{-\frac{1}{a_{11}} - ip(E)} \begin{pmatrix} 1 & 0 \\ 0 & 0 \end{pmatrix}, \tag{42}$$

which represents the single-channel scattering in channel 1. This amplitude satisfies $\det[f^{\mathrm{C}}(E)] = 0$ and does not have an inverse matrix, but is not the Flatté amplitude. In the same way, taking only $a_{11} \to 0$ results in the elastic scattering amplitude in channel 2. The limit $a_{12} \to 0$ gives the the trivial amplitude with all components being zero. In this way, none of these limits can reproduce the coupled-channel Flatté amplitude. Furthermore, setting two of the parameters zero with the remaining one being finite also results in the trivial amplitude. Therefore, in order to obtain a sensible coupled-channel amplitude, all the parameters must be simultaneously taken to be zero:

$$a_{11}, a_{12}, a_{22} \to 0. \tag{43}$$

In this case, the Contact amplitude is indefinite and the result depends on the ratios of a_{ij}.

In summary, we show that the difference between the Flatté and Contact amplitudes can be characterized by the determinant of the amplitude, $\det[f^{\mathrm{C}}(E)] \neq 0$ and $\det[f^{\mathrm{F}}(E)] = 0$. However, the Contact amplitude does

not directly reduce to the Flatté amplitude by imposing the condition $\det[f^C(E)] = 0$ with the parameters a_{11}, a_{12}, and a_{22}. In other words, $f^C(E)$ is not a suitable form to study the connection with the Flatté amplitude, although it represents the general form of the coupled-channel scattering amplitude.

III. GENERAL AMPLITUDE

In the previous section, we observe that the Flatté amplitude follows the condition $\det\left[f^F(E)\right] = 0$ and the Contact amplitude cannot directly be reduced to the Flatté amplitude. In this section, we first discuss the condition $\det[f(E)] = 0$ in relation with the renormalization procedure in the Contact amplitude, and construct an expression of the scattering amplitude in which the condition $\det[f(E)] = 0$ can be imposed by smoothly changing the parameters. We call this expression the General amplitude f^G, and show that f^G reproduces both the Contact amplitude and the Flatté amplitude in Sec. III B. We extract the scattering length in the General amplitude and compare with that of the Flatté amplitude in Sec. III C. The decomposition of the General amplitude into the pole and background terms is discussed in Sec. III D.

A. Formulation

To investigate the condition $\det\left[f^C(E)\right] = 0$ in more detail, we focus on the renormalization condition of the Contact amplitude. The first terms in the left hand side of the renormalization conditions (11)-(13) contain $\det[V_C] = c_{11}c_{22} - c_{12}^2$ in the denominator. In other words, $\det[V_C]$ must be nonzero to adopt the renormalization condition (11)-(13) that gives a_{11}, a_{12}, and a_{22}. This explains the observation in the previous section that Eq. (43) is required to achieve $\det\left[f^C(E)\right] = 0$. Therefore, to construct an amplitude which is smoothly connected to $\det\left[f^C(E)\right] = 0$, we need to modify the renormalization condition so that it is compatible with $\det[V_C] = 0$. For this purpose, we first consider the potential with two parameters c_{22} and x

$$V_G^{(0)} = \begin{pmatrix} c_{22}x & c_{22}\sqrt{x} \\ c_{22}\sqrt{x} & c_{22} \end{pmatrix}, \tag{44}$$

which is a special case of V_C with $c_{11} = c_{22}x$ and $c_{12} = c_{22}\sqrt{x}$, but at the same time the condition $\det[V_G^{(0)}] = 0$ is satisfied. Substituting $V_G^{(0)}$ into the Lippmann-Schwinger equation (27), we obtain the T-matrix as

$$T^{G(0)}(E) = \left[\frac{1}{c_{22}} + x\frac{\mu_1\Lambda}{\pi^2} + \frac{\mu_2\Lambda}{\pi^2} + x\frac{\mu_1}{2\pi}ip + \frac{\mu_2}{2\pi}ik\right]^{-1} \\ \times \begin{pmatrix} x & \sqrt{x} \\ \sqrt{x} & 1 \end{pmatrix}. \tag{45}$$

We express the renormalized T-matrix with the physical quantities A_{22}, ϵ as

$$T^{G(0)}(E) = \frac{1}{\frac{1}{A_{22}} + i\epsilon p + ik} \begin{pmatrix} \frac{2\pi}{\mu_1}\epsilon & \frac{2\pi}{\sqrt{\mu_1\mu_2}}\sqrt{\epsilon} \\ \frac{2\pi}{\sqrt{\mu_1\mu_2}}\sqrt{\epsilon} & \frac{2\pi}{\mu_2} \end{pmatrix}. \tag{46}$$

This is achieved by the renormalization conditions

$$x(\Lambda) = \frac{\mu_2}{\mu_1}\epsilon, \tag{47}$$

$$\frac{1}{c_{22}(\Lambda)} + x(\Lambda)\frac{\mu_1\Lambda}{\pi^2} + \frac{\mu_2\Lambda}{\pi^2} = \frac{\mu_2}{2\pi}\frac{1}{A_{22}}. \tag{48}$$

Taking the $\Lambda \to \infty$ limit, the renormalized scattering amplitude is obtained as

$$f^{G(0)}(E) = \frac{1}{-\frac{1}{A_{22}} - i\epsilon p - ik} \begin{pmatrix} \epsilon & \sqrt{\epsilon} \\ \sqrt{\epsilon} & 1 \end{pmatrix}. \tag{49}$$

In this way, we obtain the coupled-channel Contact amplitude with $\det[f(E)] = 0$, by imposing the condition $\det[V] = 0$ and modify the renormalization condition. On the other hand, comparing Eq. (49) and Eq. (37), we see that $f^{G(0)}(E)$ is equivalent to the Flatté amplitude up to the first order in k with the identification

$$\epsilon = \frac{1}{R}, \tag{50}$$

$$A_{22} = -\frac{R}{\alpha p_0}, \tag{51}$$

in Eq. (49). In this way, we show that there is a well-defined limit of the Contact amplitude with $\det[f(E)] = 0$, which is nothing but the Flatté amplitude. With these relations and Eq. (38), the Flatté scattering length a_F in Eq. (35) can also be written by A_{22} and ϵ as

$$a_F = \frac{1}{\frac{1}{A_{22}} + i\epsilon p_0}. \tag{52}$$

The remaining task is to construct the scattering amplitude which is smoothly connected to $f^{G(0)}(E)$. To this end, we propose the parametrization of the potential

$$V_G = \begin{pmatrix} c_{22}x & c_{22}\sqrt{x-y} \\ c_{22}\sqrt{x-y} & c_{22} \end{pmatrix}, \tag{53}$$

with real bare parameters c_{22}, x, and y. We require $x \geq y$ for the hermiticity of the Hamiltonian. The potential V_G is obtained by setting

$$c_{11} = c_{22}x, \quad c_{12} = c_{22}\sqrt{x-y}, \tag{54}$$

in V_C, and because of three independent parameters. The determinant of V_G is obtained as

$$\det[V_G] = c_{22}^2 y. \tag{55}$$

Therefore, the determinant of V_G vanishes with $y = 0$ or $c_{22} = 0$, but the latter is not of our interest because it

yields the trivial scattering. With $y = 0$, the potential becomes $V_{\mathrm{G}}^{(0)}$ in Eq. (44), which gives the Flatté amplitude. Namely, the parametrization in Eq. (53) allows one

to control $\det[V_{\mathrm{G}}]$ by the parameter y.

Next, we derive the scattering amplitude using V_{G}. Substituting V_{G} into Eq. (27), the T-matrix is obtained as

$$T^{\mathrm{G}}(E) = \frac{1}{D(E)} \begin{pmatrix} x + c_{22}y\left(\frac{\mu_2 \Lambda}{\pi^2} + \frac{\mu_2}{2\pi}ik\right) & \sqrt{x-y} \\ \sqrt{x-y} & 1 + c_{22}y\left(\frac{\mu_1 \Lambda}{\pi^2} + \frac{\mu_1}{2\pi}ip\right) \end{pmatrix}, \tag{56}$$

$$D(E) = \frac{1}{c_{22}} + x\frac{\mu_1 \Lambda}{\pi^2} + \frac{\mu_2 \Lambda}{\pi^2} + c_{22}y\frac{\mu_1\mu_2 \Lambda^2}{\pi^4} + \left(x\frac{\mu_1}{2\pi} + c_{22}y\frac{\mu_1\mu_2\Lambda}{2\pi^3}\right)ip + \left(\frac{\mu_2}{2\pi} + c_{22}y\frac{\mu_1\mu_2\Lambda}{2\pi^3}\right)ik - c_{22}y\frac{\mu_1\mu_2}{4\pi^2}pk. \tag{57}$$

which recovers Eq. (45) with $y = 0$. By introducing the Λ-dependence of $c_{22}(\Lambda), x(\Lambda)$, and $y(\Lambda)$ with the physical quantities A_{22}, ϵ, and γ as

$$c_{22}(\Lambda) = 2\pi^2 A_{22}\gamma\left(\pi\mu_1 - 2\mu_1 A_{22}\gamma\Lambda\right)$$
$$\times \left[(2\mu_2 A_{22}\gamma\Lambda - \pi\mu_2\epsilon)\left(2\mu_1 A_{22}\gamma\Lambda - \pi\mu_1\right)\right.$$
$$\left. -\pi^2\mu_1\mu_2(\epsilon - \gamma)\right]^{-1}, \tag{58}$$

$$x(\Lambda) = \frac{2\mu_2 A_{22}\gamma\Lambda - \pi\mu_2\epsilon}{2\mu_1 A_{22}\gamma\Lambda - \pi\mu_1}, \tag{59}$$

$$y(\Lambda) = \left[(2\mu_2 A_{22}\gamma\Lambda - \pi\mu_2\epsilon)\left(2\mu_1 A_{22}\gamma\Lambda - \pi\mu_1\right)\right.$$
$$\left. -\pi^2\mu_1\mu_2(\epsilon - \gamma)\right]\left(\pi\mu_1 - 2\mu_1 A_{22}\gamma\Lambda\right)^{-2}, \tag{60}$$

we obtain the scattering amplitude $f^{\mathrm{G}}(E)$ in the $\Lambda \to \infty$ limit as

$$f^{\mathrm{G}}(E) = \frac{1}{-\frac{1}{A_{22}} - i\epsilon p - ik + A_{22}\gamma pk}$$
$$\times \begin{pmatrix} \epsilon + iA_{22}\gamma k & \sqrt{\epsilon - \gamma} \\ \sqrt{\epsilon - \gamma} & 1 + iA_{22}\gamma p \end{pmatrix}. \tag{61}$$

In the following, we call $f^{\mathrm{G}}(E)$ the General amplitude. When $\gamma \neq 0$, $f^{\mathrm{G}}(E)$ has an inverse matrix, which is given by

$$\left[f^{\mathrm{G}}(E)\right]^{-1} = \begin{pmatrix} -\frac{1}{A_{22}}\frac{1}{\gamma} - ip & \frac{1}{A_{22}}\frac{\sqrt{\epsilon-\gamma}}{\gamma} \\ \frac{1}{A_{22}}\frac{\sqrt{\epsilon-\gamma}}{\gamma} & -\frac{1}{A_{22}}\frac{\epsilon}{\gamma} - ik \end{pmatrix}. \tag{62}$$

It is seen in this form that the physical parameters should satisfy $\epsilon > \gamma$ in order to be consistent with the optical theorem.

B. Relation with Contact and Flatté amplitudes

In this section, we compare the General amplitude $f^{\mathrm{G}}(E)$ with the Contact amplitude $f^{\mathrm{C}}(E)$ and the Flatté amplitude $f^{\mathrm{F}}(E)$ in terms of the parameters. First we show that $f^{\mathrm{G}}(E)$ contains both $f^{\mathrm{C}}(E)$ and $f^{\mathrm{F}}(E)$ in the
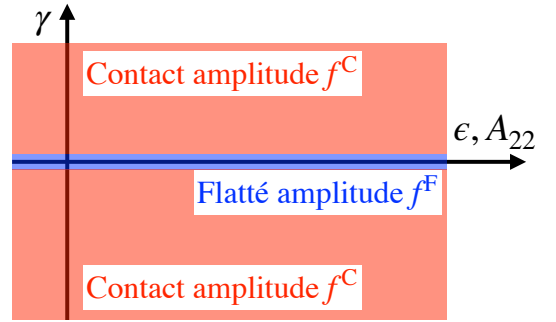

FIG. 1. Schematic illustration of the parameter space of the General amplitude f^{G} in relation with the Contact amplitude f^{C} and Flatté amplitude f^{F}.

parameter space. By comparing the inverse of the Contact amplitude Eq. (14) with that of the General amplitude (62), we find the relations

$$a_{11} = A_{22}\gamma, \tag{63}$$

$$a_{12} = \frac{A_{22}\gamma}{\sqrt{\epsilon - \gamma}}, \tag{64}$$

$$a_{22} = \frac{A_{22}\gamma}{\epsilon}. \tag{65}$$

In this case, however, the condition $\gamma \neq 0$ is imposed in the General amplitude, as mentioned above. On the other hand, imposing the condition $\gamma = 0$ on $f^{\mathrm{G}}(E)$ in Eq. (61), we obtain

$$f^{\mathrm{G}}(E; A_{22}, \epsilon, \gamma = 0) = \frac{1}{-\frac{1}{A_{22}} - i\epsilon p - ik}\begin{pmatrix} \epsilon & \sqrt{\epsilon} \\ \sqrt{\epsilon} & 1 \end{pmatrix}. \tag{66}$$

Thus, we find that $f^{\mathrm{G}}(E)$ reduces to Eq. (49) which is the Flatté amplitude up to the first order in k. Therefore, we find that the General amplitude $f^{\mathrm{G}}(E)$ with $\gamma \neq 0$ is the Contact amplitude $f^{\mathrm{C}}(E)$ and the General amplitude reduces to the Flatté amplitude at $\gamma = 0$ (see Fig. 1).

We are now in a position to revisit the relation between the Contact amplitude $f^{\mathrm{C}}(E)$ with the Flatté amplitude

$f^{\mathrm{F}}(E)$ using the parameters of the General amplitude A_{22}, ϵ, and γ. In Sec. II C, we have shown that the Contact amplitude cannot reduce to the Flatté amplitude directly. First, from Eqs. (63)-(65), the condition $\gamma = 0$ indicates that all the parameters in the Contact amplitude vanish:

$$a_{11} \to 0 \qquad (\gamma \to 0), \tag{67}$$
$$a_{12} \to 0 \qquad (\gamma \to 0), \tag{68}$$
$$a_{22} \to 0 \qquad (\gamma \to 0). \tag{69}$$

This is in fact the condition discussed in the section II C for the determinant of the Contact amplitude to vanish with the coupled-channel amplitude. Thanks to the relations (63)-(65), we can now establish the ratios of the a_{ij} parameters in the $\gamma \to 0$ limit to obtain the Flatté amplitude. For any value of γ, the following relations hold:

$$a_{11} \left(\frac{1}{a_{12}^2} - \frac{1}{a_{11}a_{22}} \right) = -\frac{1}{A_{22}}, \tag{70}$$
$$\frac{a_{11}}{a_{22}} = \epsilon. \tag{71}$$

In addition, Eqs. (63) and (64) shows that the relation

$$\frac{a_{11}}{a_{12}} \to \sqrt{\epsilon} \qquad (\gamma \to 0), \tag{72}$$

holds in the limit of $\gamma \to 0$. Rewriting the Contact amplitude in Eq. (15) as

$$f^{\mathrm{C}}(E) = \frac{1}{a_{11} \left(\frac{1}{a_{12}^2} - \frac{1}{a_{11}a_{22}} \right) - ik - i\frac{a_{11}}{a_{22}}p + a_{11}pk} \\ \times \begin{pmatrix} \frac{a_{11}}{a_{22}} + ia_{11}k & \frac{a_{11}}{a_{12}} \\ \frac{a_{11}}{a_{12}} & 1 + ia_{11}p \end{pmatrix}, \tag{73}$$

and sending all a_{ij} to zero with keeping the ratios in Eqs. (70)-(72), we find that $f^{\mathrm{C}}(E)$ reduces to

$$\lim_{a_{11}, a_{12}, a_{22} \to 0} f^{\mathrm{C}}(E) = \frac{1}{-\frac{1}{A_{22}} - ik - i\epsilon p} \begin{pmatrix} \epsilon & \sqrt{\epsilon} \\ \sqrt{\epsilon} & 1 \end{pmatrix}, \tag{74}$$

which is the Flatté amplitude in the form of $f_{\mathrm{G}}^{(0)}(E)$ in Eq. (49).

As mentioned in Sec. II C, the Contact amplitude cannot reproduce the Flatté amplitude with finite parameters a_{11}, a_{12}, and a_{22}. Here we show that the parametrization of the General amplitude with A_{22}, ϵ, and γ is suitable to smoothly connect the Contact amplitude and the Flatté amplitude. This is essential to examine the constraints in the cross sections from the Flatté amplitude by the numerical analysis in the next section. At the same time, the General amplitude clarifies the conditions (70), (70), and (72) required to obtain the Flatté amplitude from the Contact amplitude by taking the limit $a_{ij} \to 0$.

C. Scattering length

In this section, we focus on the parameter γ that characterizes the difference between the Contact amplitude and the Flatté amplitude and discuss the effect of γ on the scattering length in the General amplitude. First, we expand the General amplitude in k (momentum of channel 2) and derive the scattering length of the General amplitude. Next, we show that the constant term in the denominator of the (1,1) component f_{11}^{G} is different from the value determined by the scattering length, except for the special case $\gamma = 0$ corresponding to the Flatté amplitude.

Expanding the denominator of the (2,2) component of the General amplitude $f_{22}^{\mathrm{G}}(E)$ in Eq. (61), we obtain

$$f_{22}^{\mathrm{G}}(E) = \left[-\frac{1}{A_{22}} \left(\frac{\frac{1}{A_{22}} + i\epsilon p_0}{\frac{1}{A_{22}} + i\gamma p_0} \right) - \frac{i(\epsilon - \gamma)}{2(1 + iA_{22}\gamma p_0)^2 p_0} k^2 \right. \\ \left. - ik + \mathcal{O}(k^4) \right]^{-1}. \tag{75}$$

Because this is consistent with the effective range expansion, the scattering length of the General amplitude is defined as

$$a_{\mathrm{G}} = A_{22} \left(\frac{\frac{1}{A_{22}} + i\gamma p_0}{\frac{1}{A_{22}} + i\epsilon p_0} \right) \tag{76}$$
$$= A_{22} \frac{\frac{1}{A_{22}^2} + \epsilon\gamma p_0^2}{\frac{1}{A_{22}^2} + \epsilon^2 p_0^2} - i \frac{(\epsilon - \gamma) p_0}{\frac{1}{A_{22}^2} + \epsilon^2 p_0^2}. \tag{77}$$

Thanks to the condition $\epsilon > \gamma$, the the requirement by the optical theorem $\mathrm{Im}(a_{\mathrm{G}}) < 0$ is guaranteed in Eq. (77).

On the other hand, the (1,1) component $f_{11}^{\mathrm{G}}(E)$ gives

$$f_{11}^{\mathrm{G}}(E) = \frac{\epsilon^2}{\epsilon - \gamma} \left[-\frac{1}{A_{22}} \frac{\epsilon}{\epsilon - \gamma} - i \frac{\epsilon^2}{\epsilon - \gamma} p_0 \right. \\ \left. - \left(A_{22} \frac{\gamma}{\epsilon} + i \frac{1}{2p_0} \frac{\epsilon^2}{\epsilon - \gamma} \right) k^2 + \mathcal{O}(k^3) - ik \right]^{-1}. \tag{78}$$

As in the case of the Contact amplitude in Eq. (21), this expansion contains the odd power terms. In this way, we confirm that for $\gamma \neq 0$, only the (2,2) component of the General amplitude can be written in the form of the effective range expansion, while the (1,1) component cannot. To discuss the relation between the scattering length of the General amplitude a_{G} and that of the Flatté amplitude a_{F}, we define b_{G} from the constant term of the denominator $f_{11}^{\mathrm{G}}(E)$ in Eq. (78):

$$f_{11}^{\mathrm{G}}(E) \propto \frac{1}{-\frac{1}{b_{\mathrm{G}}} - ik + \mathcal{O}(k^2)}, \tag{79}$$

This gives $b_{\rm G}$ as

$$b_{\rm G} = \frac{(\epsilon - \gamma)\left(\frac{1}{A_{22}} - i\epsilon p_0\right)}{\epsilon\left(\frac{1}{A_{22}^2} + \epsilon^2 p_0^2\right)}$$
$$= \frac{(\epsilon - \gamma)\frac{1}{A_{22}}}{\epsilon\left(\frac{1}{A_{22}^2} + \epsilon^2 p_0^2\right)} - i\frac{(\epsilon - \gamma)p_0}{\frac{1}{A_{22}^2} + \epsilon^2 p_0^2}. \quad (80)$$

Comparison with Eq. (75) shows that the imaginary part of $b_{\rm G}$ is identical with that of $a_{\rm G}$. The real parts are, however, in general different from each other.

By setting $\gamma = 0$, the real part of $b_{\rm G}$ also coincide with that of $a_{\rm G}$. In fact, from Eqs. (75) and (80), $a_{\rm G}$ and $b_{\rm G}$ with $\gamma = 0$ are given by

$$a_{\rm G} = \frac{1}{\frac{1}{A_{22}} + i\epsilon p_0} \quad (\gamma = 0), \quad (81)$$

$$b_{\rm G} = \frac{1}{\frac{1}{A_{22}} + i\epsilon p_0} \quad (\gamma = 0). \quad (82)$$

This is natural because the General amplitude reduces to the Flatté amplitude at $\gamma = 0$. From Eq. (52), we find the relation

$$a_{\rm G} = b_{\rm G} = a_{\rm F} \quad (\gamma = 0), \quad (83)$$

which shows that both $a_{\rm G}$ and $b_{\rm G}$ reduce to the scattering length of the Flatté amplitude $a_{\rm F}$. In this way, we find that the scattering length of the Flatté amplitude $a_{\rm F}$ corresponds to the value in the special case with $\gamma = 0$. In general, the constant term $b_{\rm G}$ defined in $f_{11}^{\rm G}(E)$ is different from the scattering length $a_{\rm G}$ given in $f_{11}^{\rm G}(E)$.

D. Pole and zero of amplitude

In the previous section, it is found that the parameter γ in the General amplitude characterizes the difference between the Contact amplitude and the Flatté amplitude. In this section, we discuss the interpretation of this parameter γ, by studying the pole and zero of the amplitude. In the single-channel case, by truncating the effective range expansion in Eq. (1) up to the first order in k, the amplitude has one pole at $k = k_{\rm p} = i/a$ determined by the scattering length a. The scattering amplitude is given only by the pole term:

$$f(k) = \frac{i}{k - k_{\rm p}}. \quad (84)$$

In general, $f(k)$ has no zero unless we include a pole in the effective range expansion (Castillejo-Dalitz-Dyson zero [31–33]). For the comparison with the single-channel case, here we use the General amplitude up to the first order in k, by neglecting the k dependence in the channel 1

momentum as $p = \sqrt{(\mu_1/\mu_2)k^2 + 2\mu_1\Delta} \simeq p_0 = \sqrt{2\mu_1\Delta}$:

$$f^{\rm G}(E) = \frac{1}{-\frac{1}{A_{22}} - i\epsilon p_0 - ik + A_{22}\gamma p_0 k}$$
$$\times \begin{pmatrix} \epsilon + iA_{22}\gamma k & \sqrt{\epsilon - \gamma} \\ \sqrt{\epsilon - \gamma} & 1 + iA_{22}\gamma p_0 \end{pmatrix}. \quad (85)$$

This approximation is justified when the threshold energy difference Δ is sufficiently large.

First, we extract the pole term contribution from the General amplitude $f^{\rm G}(E)$. The General amplitude $f^{\rm G}(E)$ in Eq. (85) has only one pole at $k = k_{\rm p}^{\rm G}$:

$$k_{\rm p}^{\rm G} = \frac{\frac{1}{A_{22}} + i\epsilon p_0}{A_{22}\gamma p_0 - i} = \frac{i}{a_{\rm G}}, \quad (86)$$

which is common in all the components and determined by the scattering length $a_{\rm G}$, as in the case of the single-channel scattering. It can be seen that the pole appear near the threshold when the magnitude of the scattering length $|a_{\rm G}|$ is large. Let us rewrite each component of $f^{\rm G}(E)$ in Eq. (85) with the pole momentum $k_{\rm p}^{\rm G}$. First, $f_{22}^{\rm G}(E)$ and $f_{12}^{\rm G}(E)$ components are given by

$$f_{22}^{\rm G}(E) = \frac{i}{k - k_{\rm p}^{\rm G}}, \quad (87)$$

$$f_{12}^{\rm G}(E) = \frac{\sqrt{\epsilon - \gamma}}{1 + iA_{22}\gamma p_0}\frac{i}{k - k_{\rm p}^{\rm G}}, \quad (88)$$

which can be written only by the pole term proportional to $i/(k - k_{\rm p}^{\rm G})$. On the other hand, $f_{11}^{\rm G}(E)$ is written by

$$f_{11}^{\rm G}(E) = \frac{\epsilon - \gamma}{(1 + iA_{22}\gamma p_0)^2}\frac{i}{k - k_{\rm p}^{\rm G}} + \frac{A_{22}\gamma}{1 + iA_{22}\gamma p_0}, \quad (89)$$

which has a constant background term in addition to the pole term. In summary, $f^{\rm G}(E)$ can be decomposed into the pole term $f_{\rm p}^{\rm G}(E)$ and the background term $f_{\rm p}^{\rm G}(E)$:

$$f^{\rm G}(E) = f_{\rm p}^{\rm G}(E) + f_{\rm bg}^{\rm G}, \quad (90)$$

$$f_{\rm p}^{\rm G}(E) = \frac{i}{k - k_{\rm p}^{\rm G}}\begin{pmatrix} \frac{\epsilon - \gamma}{(1 + iA_{22}\gamma p_0)^2} & \frac{\sqrt{\epsilon - \gamma}}{1 + iA_{22}\gamma p_0} \\ \frac{\sqrt{\epsilon - \gamma}}{1 + iA_{22}\gamma p_0} & 1 \end{pmatrix}, \quad (91)$$

$$f_{\rm bg}^{\rm G} = \begin{pmatrix} \frac{A_{22}\gamma}{1 + iA_{22}\gamma p_0} & 0 \\ 0 & 0 \end{pmatrix}, \quad (92)$$

where one confirms $\det[f_{\rm p}^{\rm G}(E)] = 0$ because of the rank one nature of the pole term. As mentioned above, up to the linear order in k, the single-channel scattering amplitude (84) is given only by the pole term without the background contribution. In this sense, we can say that the appearance of the background term in the first order in momentum reflects the effect of the channel couplings. This is caused by the k dependence in the numerator of the (1,1) component of $f^{\rm G}(E)$ in Eq. (85). Therefore, the existence of the background term $f_{\rm bg}^{\rm G}$ in the General amplitude $f^{\rm G}(E)$ is a property unique to the coupled channel scattering.

Imposing the condition $\gamma = 0$ on Eq. (90), we obtain

$$f^{\mathrm{G}}(E; A_{22}, \gamma = 0, \epsilon) = \frac{i}{k - k_{\mathrm{p}}^{\mathrm{F}}} \begin{pmatrix} \epsilon & \sqrt{\epsilon} \\ \sqrt{\epsilon} & 1 \end{pmatrix}, \qquad (93)$$

where $k_{\mathrm{p}}^{\mathrm{F}} = i/A_{22} - \epsilon p_0$ is the pole of the Flatté amplitude. When $\gamma = 0$, the background term $f_{\mathrm{bg}}^{\mathrm{G}}$ disappears, because the Flatté amplitude consists of the pure pole term. This indicates that the parameter γ should be nonzero to have the background contribution. However, we see from Eq. (92) that the background term $f_{\mathrm{bg}}^{\mathrm{G}}$ depends on the parameter A_{22} as well, so the magnitude of the background is not exclusively determined by γ. Furthermore, note that the pole position $k_{\mathrm{p}}^{\mathrm{G}}$ in Eq. (86) depends on γ and therefore γ plays an important role also in the pole term.

In general, the interference between the background term and the pole term can generate zeros of the scattering amplitude [4]. Therefore, the (1,1) component of the General amplitude can have a zero point where $f_{11}^{\mathrm{G}}(E) = 0$. From Eq. (85), the momentum $k_{\mathrm{zero}}^{\mathrm{G}}$ where the amplitude vanishes is given by

$$k_{\mathrm{zero}}^{\mathrm{G}} = i \frac{1}{A_{22}} \frac{\epsilon}{\gamma}. \qquad (94)$$

Since A_{22}, ϵ, and γ are the real parameters, we find that $k_{\mathrm{zero}}^{\mathrm{G}}$ is pure imaginary. Therefore, in terms of the energy variable, the zero point appears below the threshold. Furthermore, physical scattering below the threshold of channel 2 corresponds to the imaginary axis of the upper half of the complex k-plane $\mathrm{Im}(k) > 0$. Therefore, the zero point of $f_{11}^{\mathrm{G}}(E)$ appears in the physical scattering region only if $\mathrm{Im}(k_{\mathrm{zero}}^{\mathrm{G}}) > 0$. On the other hand, the Flatté amplitude (General amplitude with $\gamma = 0$) has no zero point because there is no background contribution. This is reflected in Eq. (94) which shows that $|k_{\mathrm{zero}}^{\mathrm{G}}| \to \infty$ and the zero point disappears in the limit $\gamma \to 0$.

We have seen that the (1,1) component of the general amplitude has a zero point, which is absent in the Flatté amplitude. Therefore, if the experimental data contains a zero point in the physical energy region $\mathrm{Im}(k) > 0$ near the threshold, the analysis with the Flatté amplitude would fail to reproduce the data. In Sec. IV, we quantitatively compare the Flatté amplitude with the General amplitude in terms of the scattering cross section when $k_{\mathrm{zero}}^{\mathrm{G}}$ appears in the physical region near the threshold.

IV. NUMERICAL ANALYSIS

In this section, by using the General amplitude, we examine the behavior of the total cross sections when a resonance pole of the scattering amplitude locates near the threshold of channel 2. Here, we investigate the behavior of the scattering cross section by varying γ with the scattering length a_{G} fixed. In this way, it is possible to compare the Flatté amplitude $\gamma = 0$ with the general

case $\gamma \neq 0$, having the same amplitude at the threshold. First, in Sec. IV A, we study the parameter regions of A_{22} and ϵ when γ varies for a fixed a_{G}. Next, we summarize the actual values of the parameters used in the numerical calculation in Sec. IV B. Finally, in Sec. IV C, we discuss the behavior of the scattering cross section numerically.

A. Parameter regions

The General amplitude $f^{\mathrm{G}}(E)$ in Eq. (61) has three real parameters A_{22}, ϵ, and γ. We write the real and imaginary parts of the scattering length a_{G} in Eq. (77) as

$$a_{\mathrm{G}} = \alpha + i\beta, \qquad (95)$$

using the real constants α and β, with the condition $\beta < 0$. Because α and β are given by A_{22}, ϵ, and γ, when we fix a_{G}, A_{22} and ϵ are determined from α, β, and γ. Since the relation between the parameters and the scattering length is not linear, we first discuss the behavior of the remaining two parameters A_{22}, ϵ when the scattering length a_{G} is fixed.

Substituting the expression of the scattering length a_{G} (76) into Eq. (95), we obtain

$$1 + iA_{22}\gamma p_0 = \frac{\alpha}{A_{22}} - \epsilon\beta p_0 + i\left(\frac{\beta}{A_{22}} + \epsilon\alpha p_0\right). \qquad (96)$$

The real and imaginary parts of Eq. (96) yields the following two conditions:

$$1 = \frac{\alpha}{A_{22}} - \epsilon\beta p_0, \qquad (97)$$

$$A_{22}\gamma p_0 = \frac{\beta}{A_{22}} + \epsilon\alpha p_0. \qquad (98)$$

Solving Eq. (97) for ϵ, we obtain

$$\epsilon = \frac{1}{\beta p_0}\left(\frac{\alpha}{A_{22}} - 1\right). \qquad (99)$$

We eliminate ϵ by substituting Eq. (99) into Eq. (98). This gives a quadratic equation of A_{22}, whose two solutions are

$$A_{22}^{\pm} = \frac{-\frac{\alpha}{\beta} \pm \sqrt{\left(\frac{\alpha}{\beta}\right)^2 + 4\gamma p_0\left(\beta + \frac{\alpha^2}{\beta}\right)}}{2\gamma p_0}. \qquad (100)$$

This gives the expression of the parameter A_{22} in terms of α, β, and γ. Corresponding ϵ is obtained from Eq. (99) as

$$\epsilon^{\pm}(\alpha, \beta, \gamma) = \frac{1}{\beta p_0}\left(\frac{\alpha}{A_{22}^{\pm}(\alpha, \beta, \gamma)} - 1\right), \qquad (101)$$

In this way, there are two parameter sets $(A_{22}^{+}, \epsilon^{+}, \gamma)$ and $(A_{22}^{-}, \epsilon^{-}, \gamma)$ for a given scattering length a_{G}. To have a

real parameter A_{22}, the quantity in the square root in Eq. (100) must be nonnegative, leading to the condition among parameters

$$\left(\frac{\alpha}{\beta}\right)^2 + 4\gamma p_0\left(\beta + \frac{\alpha^2}{\beta}\right) \geq 0. \qquad (102)$$

Furthermore, considering $\beta < 0$ required by the unitarity, we obtain the following condition for γ:

$$\frac{\left(\frac{\alpha}{\beta}\right)^2}{4p_0\left(|\beta| + \frac{\alpha^2}{|\beta|}\right)} \geq \gamma. \qquad (103)$$

This shows that the range of the parameter γ has an upper bound

$$\gamma_{\mathrm{max}} = \frac{\left(\frac{\alpha}{\beta}\right)^2}{4p_0\left(|\beta| + \frac{\alpha^2}{|\beta|}\right)}, \qquad (104)$$

to reproduce the given scattering length a_{G}. We note that the inequality (102) is saturated at $\gamma = \gamma_{\mathrm{max}}$ leading to $A_{22}^+ = A_{22}^-$ and $\epsilon^+ = \epsilon^-$. In other words, the two parameter sets $(A_{22}^+, \epsilon^+, \gamma)$ and $(A_{22}^-, \epsilon^-, \gamma)$ are continuously connected at $\gamma = \gamma_{\mathrm{max}}$.

B. Setup

To examine the behavior of A_{22} and ϵ numerically, we consider the $\pi\pi$-$K\bar{K}$ system as an example. Since the threshold of $K\bar{K}$ (~ 990 MeV) is far from that of $\pi\pi$ (~ 280 MeV), we use the relativistic expression of the momentum

$$k = \sqrt{\frac{(E + 2m_K)^2}{4} - m_K^2}, \qquad (105)$$

$$p = \sqrt{\frac{(E + 2m_K)^2}{4} - m_\pi^2}. \qquad (106)$$

In this case, the momentum p at the threshold of channel 2 is evaluated as $p_0 = \sqrt{m_K^2 - m_\pi^2}$. The hadron masses are taken from PDG [3].

First, we fix the scattering length as

$$a_{\mathrm{G}} = +1.0 - i0.8 \quad \text{fm}, \qquad (107)$$

which is a typical value found in the experimental analysis [13]. By Eq. (86), the pole of $f_0(980)$ is estimated as

$$k_{\mathrm{p}}^{\mathrm{G}} = -0.095 + i0.125 \text{ GeV}, \qquad (108)$$

$$E_{\mathrm{p}}^{\mathrm{G}} = \frac{[k_{\mathrm{p}}^{\mathrm{G}}]^2}{m_K} = -0.014 - i0.048 \text{ GeV}. \qquad (109)$$

Because the imaginary part of the eigenmomentum is positive, this pole represent the quasibound state [34].

Note however that the pole position in Eq. (86) is obtained by approximating $p \sim p_0$, and the exact pole of the amplitude calculated with $p(k)$ depends not only on a_{G} but also γ. In the following calculations, we have checked that the exact pole is found within a few MeV region from the above values. Also, the upper bound γ_{max} in Eq. (104) is given by

$$\gamma_{\mathrm{max}} = 0.079. \qquad (110)$$

Numerical plots of A_{22}^+ (solid line) and A_{22}^- (dashed line) for $-1.0 \leq \gamma \leq \gamma_{\mathrm{max}}$ are shown in Fig. 2(a). As expected, two lines coincide with each other at $\gamma = \gamma_{\mathrm{max}}$. From Fig. 2(a), we find that while A_{22}^- has a finite value at $\gamma = 0$, A_{22}^+ diverges as $A_{22}^+ \to \pm\infty$ with $\gamma \to 0^\pm$. That is, for $a_{\mathrm{G}} = +1.0 - i0.8$ [fm], the Flatté amplitude is obtained by adopting the solution A_{22}^- and setting $\gamma \to 0$. Next, the plots of $\epsilon^\pm$ as functions of γ are shown in Fig. 2(b). The solid line represents ϵ^+ and the dashed line ϵ^-. From Fig. 2(b), we can see that ϵ^+ is always positive in this range of γ, while the sign of ϵ^- changes around $\gamma \sim -0.4$. This property will be discussed in relation with the zero point of the scattering cross section. It can be checked that the condition $\epsilon > \gamma$ is satisfied for both solutions in this parameter region.

It is instructive to consider the case with the scattering length having the opposite sign of the real part from Eq. (107). For this purpose, we also examine

$$a_{\mathrm{G}} = -1.0 - i0.8 \quad \text{fm}. \qquad (111)$$

Corresponding pole position of $f_0(980)$ in Eq. (86) is found to be

$$k_{\mathrm{p}}^{\mathrm{G}} = -0.095 - i0.125 \text{ GeV}, \qquad (112)$$

$$E_{\mathrm{p}}^{\mathrm{G}} = -0.014 + i0.048 \text{ GeV}. \qquad (113)$$

Negative imaginary part of the eigenmomentum suggests that this pole would be a virtual state in the absence of the coupling to the $\pi\pi$ channel. According to Ref. [34] we call this the quasivirtual state. Because γ_{max} in Eq. (104) is invariant under $\alpha \to -\alpha$, the value in Eq. (110) still holds in the present case. We plot A_{22} and ϵ as functions of γ in Fig. 3. Comparing $A_{22}^\pm$ in Fig. 2(a) with those in Fig. 3(a) we notice that there is some symmetry. In fact, from Eq. (100), we find the relation $A_{22}^\pm(-\alpha) = -A_{22}^\mp(\alpha)$ under the sign flip of the real part of the scattering length, which explains the behaviors in Fig. 2(a) and Fig. 3(a). This suggests that the Flatté amplitude is obtained by adopting A_{22}^+ and setting $\gamma \to 0$ for $a_{\mathrm{G}} = -1.0 - i0.8$ fm. The behaviors of $\epsilon^\pm$ in Figs 2(b) and 3(b) can also be explained by the relation $\epsilon^\pm(-\alpha) = \epsilon^\mp(\alpha)$ which follows from Eq. (101) and the property of $A_{22}^\pm$.

C. Total cross sections

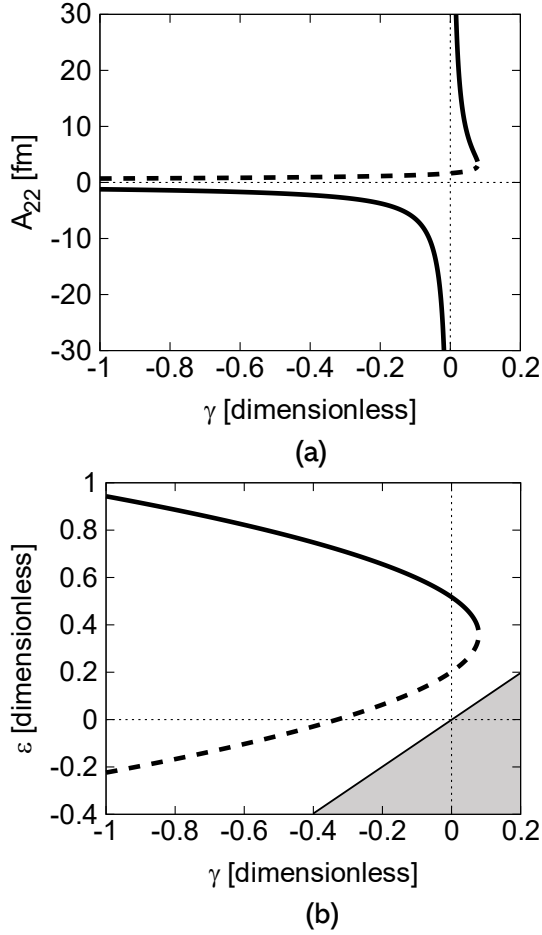In the previous section, we established the behaviors of A_{22} and ϵ when the scattering length a_{G} is fixed and

(a)

(b)

FIG. 2. Parameters A_{22} (a) and ϵ (b) as functions of γ with the scattering length $a_{\mathrm{G}} = +1.0 - i0.8$ fm. The solid (dashed) lines represent A_{22}^+ and ϵ^+ (A_{22}^- and ϵ^-). The shaded area is excluded by the condition $\epsilon > \gamma$ by the optical theorem.

γ is varied. In this section, we discuss the behavior of the scattering cross section with representative values of the parameters. In the near threshold region where the s-wave contribution dominates, the total cross section $\sigma_{ij}(E)$ is given by

$$\sigma_{ij}(E) = 4\pi \frac{p_i}{p_j} |f_{ij}(E)|^2. \tag{114}$$

Because the cross section is proportional to $|f_{ji}(E)|^2$, in this section, we use

$$\sigma_{ij}^{\mathrm{N}}(E) \equiv |f_{ij}(E)|^2 / |f_{ij}(0)|^2, \tag{115}$$

which is normalized at the threshold.

Before performing the numerical analysis, let us examine the analytic properties of $\sigma_{ij}^{\mathrm{N}}(E)$. From Eq. (85), the (1,1) component of the cross section $\sigma_{11}^{\mathrm{N}}(E)$ is given by

$$\sigma_{11}^{\mathrm{N}}(E) = \left| \frac{1 + i\frac{A_{22}\gamma}{\epsilon}k}{1 + ia_{\mathrm{G}}k} \right|^2, \tag{116}$$

(a)

(b)
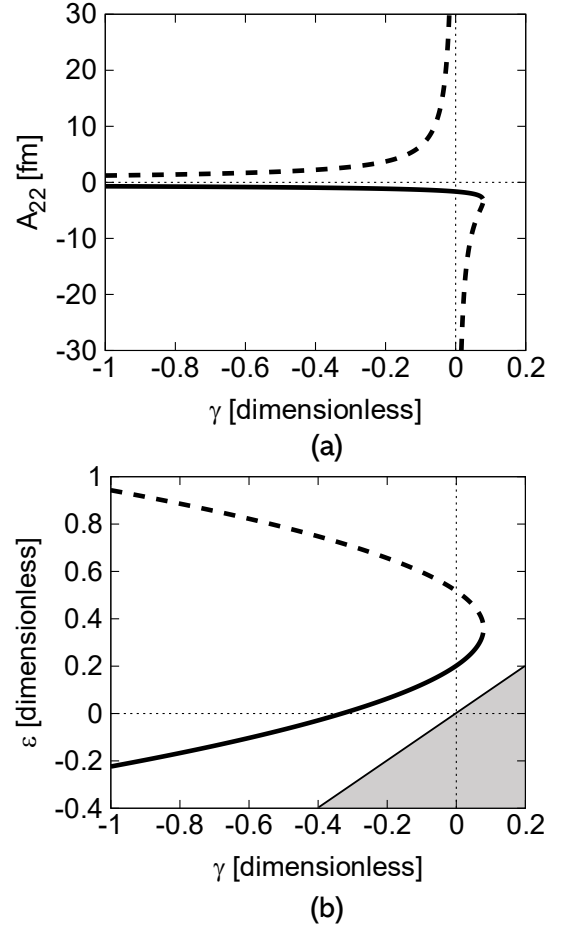
FIG. 3. Same as Fig. 2 but with $a_{\mathrm{G}} = -1.0 - i0.8$ fm.

which depends on three parameters A_{22}, ϵ, and γ. Thus, even if we fix the scattering length a_{G}, the cross section still depends on the parameter γ. In contrast, the (1,2) and (2,2) components of the normalized cross section $\sigma^{\mathrm{N}}(E)$ are given by

$$\sigma_{12}^{\mathrm{N}}(E) = \sigma_{22}^{\mathrm{N}}(E) = \left| \frac{1}{1 + ia_{\mathrm{G}}k} \right|^2. \tag{117}$$

which depends exclusively on the scattering length a_{G}. In other words, they are independent of γ when a_{G} is fixed. In this way, the γ dependence of the normalized cross section exists only in the (1,1) component, because only $f_{11}^{\mathrm{G}}(E)$ contains the background term as discussed in Sec. III D.

Now we calculate the normalized cross sections near the threshold of channel 2 by varying γ with the scattering length a_{G} being fixed. We focus on $\sigma_{11}^{\mathrm{N}}(E)$ that has γ dependence for a fixed a_{G}. First, we set

$$a_{\mathrm{G}} = +1.0 - i0.8 \quad \mathrm{fm}$$

Because γ should be smaller than $\gamma_{\max}$, we choose $\gamma = 0.07, 0.00, -0.01, -10.0$ as representative values. The corresponding parameters $A_{22}^\pm$ and $\epsilon^\pm$ are shown in Ta-

TABLE I. Parameters $A_{22}^{\pm}$ and $\epsilon^{\pm}$ for $a_{\mathrm{G}} = +1.0 - i0.8$ fm.

γ	A_{22}^{+} (fm)	ϵ^{+}	A_{22}^{-} (fm)	ϵ^{-}
$+0.07$	$+4.95$	$+0.41$	$+2.45$	$+0.31$
0.00	-	$+0.52$	$+1.64$	$+0.20$
-0.01	-53.4	$+0.53$	$+1.59$	$+0.19$
-10.0	-0.32	$+2.14$	$+0.27$	-1.42
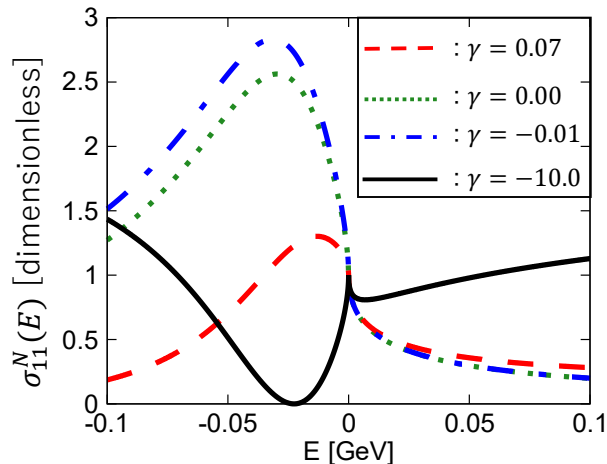
FIG. 4. The (1,1) component of the normalized cross sections $\sigma_{11}^{\mathrm{N}}(E) = |f_{11}^{\mathrm{G}}(E)|^2/|f_{11}^{\mathrm{G}}(0)|^2$ as functions of the energy E. The scattering length is fixed as $a_{\mathrm{G}} = +1.0 - i1.0$ fm and the solution with A_{22}^{-} and ϵ^{-} is chosen. The parameter is $\gamma = 0.07$ (dashed line), $\gamma = 0.00$ (dotted line), $\gamma = -0.01$ (dash-dotted line), and $\gamma = -10.0$ (solid line).

ble I. The Flatté amplitude corresponds to the solution with A_{22}^{-} and ϵ^{-} at $\gamma = 0$.

Choosing A_{22}^{-} and ϵ^{-}, we plot the (1,1) component of the cross section $\sigma_{11}^{\mathrm{N}}(E)$ for four values of γ in Fig. 4. The dotted line ($\gamma = 0$) corresponds to the cross section by the Flatté amplitude which shows the peak structure below the threshold. This is because in this amplitude there is a quasibound state below the threshold, as discussed above. The peak locates around $E \sim -0.03$ GeV, which is shifted from the real part of the pole energy ~ -0.01 GeV due to the threshold effect. When γ is increased from zero, the peak structure remains, but the size of the peak becomes smaller than that with $\gamma = 0$, as seen by the dashed line ($\gamma = 0.07$). The peak position moves toward the threshold. On the other hand, the peak becomes larger when γ is slightly decreased from zero in the negative direction ($\gamma = -0.01$, dash-dotted line). In this way, the cross sections with small $|\gamma|$ have a peak structure, for which the Flatté amplitude can be used to fit the data. However, if we fit the peaks of, for instance, the dashed or dash-dotted lines in Fig. 4 using the Flatté amplitude, the scattering length would be different from the exact value $+1.0 - i0.8$ fm. Because the value of γ is not known in advance in the experimental data, the scattering length extracted by the Flatté amplitude might be

deviated from the exact value.

When we adopt a large and negative $\gamma = -10.0$ (solid line in Fig. 4), the cross section $\sigma_{11}^{\mathrm{N}}(E)$ no longer shows the peak structure but exhibits a dip structure instead, in sharp contrast to the other cases. In the present case, at the bottom of this dip, the cross section $\sigma_{11}^{\mathrm{N}}(E)$ becomes exactly zero, meaning that the scattering amplitude vanishes at that energy. This is the manifestation of the Castillejo-Dalitz-Dyson zero [31–33], caused by the interference between the pole and background, as discussed in Sec. III D. From Eq. (94), the zero point of the (1,1) component $f_{11}^{\mathrm{G}}(E)$ of the General amplitude is calculated as

$$k_{\mathrm{zero}}^{\mathrm{G}} = i0.10 \text{ GeV}, \tag{118}$$

$$E_{\mathrm{zero}}^{\mathrm{G}} = \frac{[k_{\mathrm{zero}}^{\mathrm{G}}]^2}{m_K} = -0.02 \text{ GeV}. \tag{119}$$

In fact, the zero point of the cross section indeed occurs in Fig. 4 at the value of Eq. (119). When the cross section shows the dip structure as the solid line ($\gamma = -10.0$) in Fig. 4, the Flatté amplitude does not work. As shown in Sec. III D, there is no zero point in the Flatté amplitude, and thus no zero of the cross section occurs. In addition, the typical Flatté amplitude exhibits either the peak structure or the threshold cusp structure [21]; the former corresponds to the dotted line in Fig. 4 and the latter to the cross section with $a_{\mathrm{G}} = -1.0 - i0.8$ fm discussed below. These structures are clearly different from the dip structure shown by the solid line ($\gamma = -10.0$) in Fig. 4. In contrast to the typical cross sections, the solid line in Fig. 4 does not show the peak nor cusp, even though the pole is near the threshold. This result indicates that the analysis of the exotic hadrons requires a detailed study of the behavior of the scattering cross section near the threshold, rather than focusing only on peaks and cusp (see also Refs. [29, 35]).

In general, the zero point appears in the physical region when $\epsilon/(A_{22}\gamma) > 0$. From Fig. 2, this corresponds to $\gamma \lesssim -0.4$ ($A_{22}^{-} > 0, \epsilon^{-} < 0, \gamma < 0$) or $0 < \gamma < \gamma_{\mathrm{max}}$ ($A_{22}^{-} > 0, \epsilon^{-} > 0, \gamma > 0$). Therefore, the dashed line ($\gamma = 0.07$) in Fig. 4 also has a zero point somewhere in the $E < 0$ region, but the dash-dotted line ($\gamma = -0.01$) does not. As discussed in Eq. (94), when γ is small, the corresponding momentum becomes large and the zero point appears far from the threshold. In fact, the zero point energy for $\gamma = 0.07$ is $E = -0.25$ GeV which locates outside of the figure.

The results with A_{22}^{+} and ϵ^{+} are shown in Fig. 5. The case with $\gamma = 0$ is not shown because A_{22}^{+} diverges. As mentioned in Sec. IV A, A_{22}^{+} and ϵ^{+} are continuously connected with A_{22}^{-} and ϵ^{-} at $\gamma = \gamma_{\mathrm{max}}$, so the dashed line with $\gamma \sim \gamma_{\mathrm{max}}$ in Fig. 5 shows a smaller peak structure than the dashed line in Fig. 4. In Fig. 5, when $\gamma = -0.01$ (dash-dotted line) the peak structure of the cross section is almost invisible. When γ is further decreased down to $\gamma = -10.0$ (solid line), the zero point appears in the physical region below the threshold, generating a sharp dip structure. It can be seen from Fig. 2 that the zero
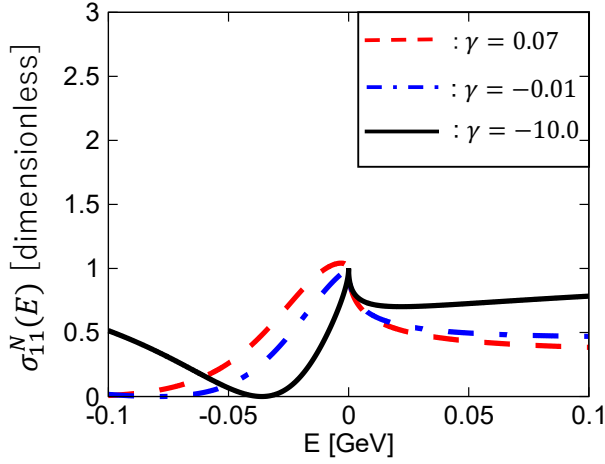
FIG. 5. Same as Fig. 2 but with A_{22}^+ and ϵ^+.
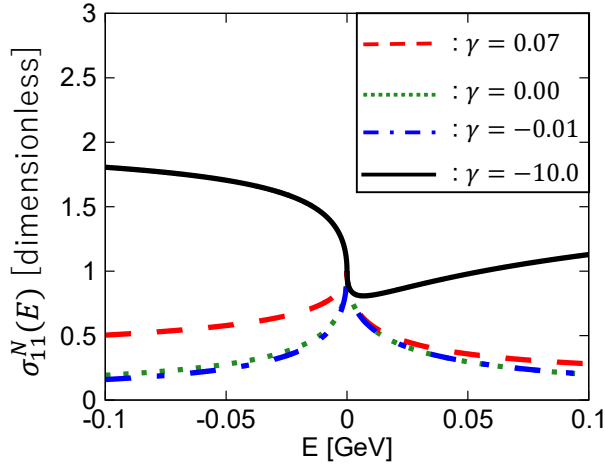
FIG. 6. Same as Fig. 2 but the scattering length is fixed as $a_{\rm G} = -1.0 - i0.8$ fm with A_{22}^+ and ϵ^+.

point is always in the physical region irrespective to the value of γ, since the relations $\epsilon^+ > 0$ and $A_{22}^+\gamma > 0$ always hold. The results in Fig. 5 show that if the zero point is far enough from the threshold with small $|\gamma|$, the peak structure is preserved, but if the zero point appears near the threshold with large $|\gamma|$, the dip structure is produced. Note also that the solid line in Fig. 5 shows a cusp at the threshold, even though the amplitude has a quasibound pole. This is again peculiar feature in the General amplitude, which cannot be reproduced by the Flatté amplitude.

Next, we discuss the cross sections with the scattering length

$$a_{\rm G} = -1.0 - i0.8 \text{ fm.} \qquad (120)$$

The corresponding parameters $A_{22}^{\pm}$ and $\epsilon^{\pm}$ for $\gamma = 0.07$, 0.00, -0.01, -10.0 are shown in Table. II. Choosing A_{22}^+ and ϵ^+, we plot the normalized cross sections $\sigma_{11}^{\rm N}(E)$ with $\gamma = 0.07$, 0.00, -0.01, -10.0 in Fig. 6. With $\gamma = 0$ (Flatté amplitude), the cross section shows

TABLE II. Parameters $A_{22}^{\pm}$ and $\epsilon^{\pm}$ for $a_{\rm G} = -1.0 - i0.8$ fm.

γ	A_{22}^+ (fm)	ϵ^+	A_{22}^- (fm)	ϵ^-
$+0.07$	-2.45	$+0.31$	-4.95	$+0.41$
0.00	-1.64	$+0.20$	-	$+0.52$
-0.01	-1.59	$+0.19$	$+53.4$	$+0.53$
-10.0	-0.27	-1.42	-0.32	$+2.14$
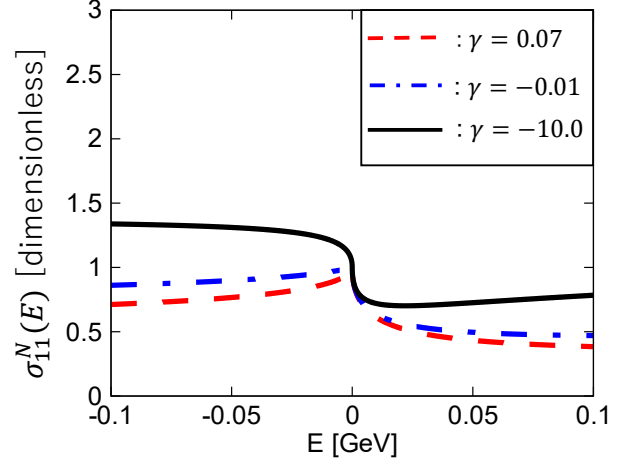
FIG. 7. Same as Fig. 6 but with A_{22}^- and ϵ^-.

a threshold cusp structure. Because the pole of the quasivirtual state is not on the most adjacent Riemann sheet to the physical scattering, it does not create a peak structure of the cross section. The existence of the quasivirtual pole near the threshold is considered to strengthen the effect of the threshold cusp. When γ is increased, as shown by the dashed line ($\gamma = 0.07$), $\sigma_{11}^{\rm N}(E)$ becomes slightly enhanced, in particular in the region below the threshold. On the other hand, when γ is slightly decreased, $\sigma_{11}^{\rm N}(E)$ is suppressed, as seen in the dash-dotted line ($\gamma = -0.01$). In both cases, the shape of $\sigma_{11}^{\rm N}(E)$ is modified from the Flatté amplitude only slightly, but the cusp structure is maintained. However, with a large negative $\gamma = -10.0$ (solid line), the cross section shows a qualitatively different behavior. One finds that the cusp at the threshold disappears due to the sign flip of the slope of the cross section below the threshold. Because of this, the cross section shows a small dip structure above the threshold. This dip structure is not caused by the zero point of the scattering amplitude, but it exhibits the local minimum of $\sigma_{11}^{\rm N}(E)$. It is clear that that the Flatté amplitude cannot reproduce the cross section with the dip similar to the solid line.

The cross sections $\sigma_{11}^{\rm N}(E)$ with A_{22}^- and ϵ^- are plotted in Fig. 7 for $\gamma = 0.07$, -0.01, and -10.0. The cross section shows the cusp structure for $\gamma = 0.07$ (dashed line) and $\gamma = -0.01$ (dash-dotted line), with a slightly enhanced strength. When γ is taken as large and negative value ($\gamma = -10.0$), a dip appears above the threshold instead of the cusp.

With the Flatté amplitude, the cross section shows a peak below the threshold for $\mathrm{Re}(a_\mathrm{F}) > 0$ or a cusp at the threshold for $\mathrm{Re}(a_\mathrm{F}) < 0$. From the above results, we find that the shape of the elastic scattering cross section in channel 1 can be changed significantly from these typical behaviors by varying γ. In particular, if γ is large and negative, the peak can be changed into a cusp even with $\mathrm{Re}(a_\mathrm{G}) > 0$, and $\sigma_{11}^\mathrm{N}(E)$ can have a dip near the threshold. Therefore, in analyzing the scattering near the threshold, it is important to perform analysis paying attention to the peak, cusp, and dip structures, rather than simply fitting the data by the Flatté amplitude [29, 35].

V. SUMMARY

In this paper, we discuss the behavior of the coupled-channel scattering amplitude near the higher energy threshold by constructing the General amplitude with new parametrization. First, in Sec. II, we introduce the Contact amplitude and Flatté amplitude based on the effective field theory. Through the comparison of two amplitudes, we show that the origin of the problem of the number of parameters in the Flatté amplitude near the threshold [21] can be traced back to the vanishing of the determinant of the scattering amplitude. It is also shown that the standard parametrization with three parameters a_{ij} in the Contact amplitude is not suitable to smoothly connect to the Flatté amplitude.

Based on this observation, we modify the renormalization conditions in the effective field theory and construct the General amplitude with three alternative parameters, A_{22}, ϵ, and γ. With $\gamma \neq 0$, the General amplitude has one-to-one correspondence with the Contact amplitude, and it directly reduces to the Flatté amplitude at $\gamma = 0$. Namely, the General amplitude allows us to examine how the Contact amplitude approaches the Flatté amplitude by varying the parameter γ. It is also shown in the General amplitude that the scattering length is defined in the (2,2) component (higher energy channel), which is in general different from the constant term in the denominator of the (1,1) component (lower energy channel), except for the special case of $\gamma = 0$ corresponding to the Flatté amplitude. Finally, we show that the (1,1) component of the General amplitude contains the background term in addition to the pole term, even in the linear order in the momentum. Since the background term disappears at $\gamma = 0$, the parameter γ is considered to control the existence of the background. It is shown that the background term can cause the zero of the amplitude by the interference with the pole term.

Finally, the behavior of the scattering cross section of the General amplitude is numerically studied by varying γ with the scattering length being fixed. For a small $|\gamma|$, the cross section shows either the peak structure or the threshold cusp structure, as typically observed in the Flatté amplitude. It is however shown that the scattering length obtained from the analysis by the Flatté am-plitude may quantitatively deviate from the exact value, due to the contribution from the background term. It is also found that by enhancing the background contribution with large and negative γ, a dip structure can be caused by the zero of the scattering amplitude (see also Refs. [29, 35]), which cannot be reproduced by the simple Flatté amplitude. In such cases, the threshold cusp structure may appear even when the real part of the scattering length is positive.

The general amplitude proposed in this study should be useful to extract the scattering length and pole position of the near-threshold exotic hadrons through the analysis of the experimental data. Since the actual exotic hadrons are often coupled to three or more channels, the extension of the General amplitude for multi-channel scattering serves as a future prospect. To enlarge the applicability of the framework, it is necessary to include the higher-order terms in the effective field theory, which also gives precise determination of the effective range. With these extensions, we expect that the application of the General amplitude to the actual experimental data will help to accurately determine the properties of the exotic hadrons near the threshold.

Appendix A: N channel scattering

Here we compare the number of independent parameters in the near-threshold Contact and Flatté amplitudes in the two-body scattering with N channels. With a straightforward generalization of Sec. II A, the N channel Contact amplitude reads

$$[f^\mathrm{C}(E)]^{-1} = \begin{pmatrix} -\frac{1}{a_{11}} - ip_1 & \frac{1}{a_{12}} & \cdots & -\frac{1}{a_{1N}} \\ \frac{1}{a_{12}} & -\frac{1}{a_{22}} - ip_2 & \cdots & \frac{1}{a_{2N}} \\ \vdots & \vdots & \ddots & \vdots \\ -\frac{1}{a_{1N}} & \frac{1}{a_{2N}} & \cdots & -\frac{1}{a_{NN}} - ip_N \end{pmatrix},$$

(A1)

where p_j is the momentum in channel j. The amplitude $f^\mathrm{C}(E)$ contains $N(N+1)/2$ independent parameters a_{ij}.

TABLE III. Number of independent parameters in the Contact amplitude (A1) and the Flatté amplitude (A3).

Channel	2	3	N
Contact (A1)	3	6	$N(N+1)/2$
Flatté (A3)	2	3	N
Conditions	1	3	$N(N-1)/2$

The Flatté amplitude with N channels can be written as

$$f^{\mathrm{F}}(E) = \frac{1}{2E_{\mathrm{BW}} - 2E - i\sum_{j=1}^{N} g_j^2 p_j}$$

$$\times \begin{pmatrix} g_1^2 & g_1 g_2 & \cdots & g_1 g_N \\ g_1 g_2 & g_2^2 & \cdots & g_2 g_N \\ \vdots & \vdots & \ddots & \vdots \\ g_1 g_N & g_2 g_N & \cdots & g_N^2 \end{pmatrix}, \qquad (A2)$$

which contains N coupling constants $g_j(j = 1, \cdots N)$ and one bare energy E_{BW}, so there are $N + 1$ independent parameters in total. Near the threshold of channel 1, by neglecting the terms with p_1^2 or higher, we obtain

$$f^{\mathrm{F}}(E) \sim \frac{1}{\alpha - ip_1 - i\sum_j r_j p_j^{(0)}}$$

$$\times \begin{pmatrix} 1 & \sqrt{r_2} & \cdots & \sqrt{r_N} \\ \sqrt{r_2} & r_2 & \cdots & \sqrt{r_2 r_N} \\ \vdots & \vdots & \ddots & \vdots \\ \sqrt{r_N} & \sqrt{r_2 r_N} & \cdots & r_N \end{pmatrix}, \qquad (A3)$$

where we define

$$\frac{g_j^2}{g_1^2} = R_j, \qquad \frac{2E_{\mathrm{BW}}}{g_1^2} = \alpha, \qquad (A4)$$

$$p_j^{(0)} = p_j(p_1 = 0), \qquad (A5)$$

In this case, the amplitude has N parameters, $r_j(j = 2, \cdots, N)$ and α.

As summarized in Table III, the Contact amplitude always has a larger number of parameters. Namely, there should be

$$\frac{1}{2}N(N-1), \qquad (A6)$$

conditions imposed on the Flatté amplitude, as in the case of two-channel scattering. This is achieved by demanding all the cofactors of the off-diagonal components vanish.

[1] F.-K. Guo, C. Hanhart, U.-G. Meißner, Q. Wang, Q. Zhao, and B.-S. Zou, Hadronic molecules, Rev. Mod. Phys. **90**, 015004 (2018), [Erratum: Rev.Mod.Phys. 94, 029901 (2022)], arXiv:1705.00141 [hep-ph].

[2] N. Brambilla, S. Eidelman, C. Hanhart, A. Nefediev, C.-P. Shen, C. E. Thomas, A. Vairo, and C.-Z. Yuan, The XYZ states: experimental and theoretical status and perspectives, Phys. Rept. **873**, 1 (2020), arXiv:1907.07583 [hep-ex].

[3] R. L. Workman et al. (Particle Data Group), Review of Particle Physics, PTEP **2022**, 083C01 (2022).

[4] J. R. Taylor, Scattering Theory: The Quantum Theory on Nonrelativistic Collisions (Wiley, New York, 1972).

[5] T. Hyodo and M. Niiyama, QCD and the strange baryon spectrum, Prog. Part. Nucl. Phys. **120**, 103868 (2021), arXiv:2010.07592 [hep-ph].

[6] S. M. Flatte, Coupled - Channel Analysis of the $\pi\eta$ and $K\bar{K}$ Systems Near $K\bar{K}$ Threshold, Phys. Lett. B **63**, 224 (1976).

[7] D. V. Bugg, V. V. Anisovich, A. Sarantsev, and B. S. Zou, Coupled channel analysis of data on $\bar{p}p \to 3\pi^0, \eta\eta\pi^0$, and $\eta\pi^0\pi^0$ at rest, with the N/D method, Phys. Rev. D **50**, 4412 (1994).

[8] S. Teige et al. (E852), Properties of the $a^0(980)$ meson, Phys. Rev. D **59**, 012001 (1999), arXiv:hep-ex/9608017.

[9] M. N. Achasov et al., The $\phi \to \eta\pi^0\gamma$ decay, Phys. Lett. B **479**, 53 (2000), arXiv:hep-ex/0003031.

[10] M. N. Achasov et al., The $\phi(1020) \to \pi^0\pi^0\gamma$ decay, Phys. Lett. B **485**, 349 (2000), arXiv:hep-ex/0005017.

[11] J. M. Link et al. (FOCUS), Study of the $D^0 \to$ $K^+K^-\pi^+\pi^-$ decay, Phys. Lett. B **610**, 225 (2005), arXiv:hep-ex/0411031.

[12] M. Ablikim et al. (BES), Resonances in $J/\psi \to \phi\pi^+\pi^-$ and ϕK^+K^-, Phys. Lett. B **607**, 243 (2005), arXiv:hep-ex/0411001.

[13] F. Ambrosino et al. (KLOE), Study of the decay $\phi \to$ $f^0(980)\gamma \to \pi^+\pi^-\gamma$ with the KLOE detector, Phys. Lett. B **634**, 148 (2006), arXiv:hep-ex/0511031.

[14] A. Garmash et al. (Belle), Evidence for Large Direct CP Violation in $B^{\pm} \to \rho(770)^0 K^{\pm}$ from Analysis of Three-body Charmless $B^{\pm} \to K^{\pm}\pi^{\pm}\pi^{\pm}$ Decays, Phys. Rev. Lett. **96**, 251803 (2006), arXiv:hep-ex/0512066.

[15] F. Ambrosino et al. (KLOE), Dalitz plot analysis of $e^+e^- \to \pi^0\pi^0\gamma$ events at $\sqrt{s} \simeq M_\phi$ with the KLOE detector, Eur. Phys. J. C **49**, 473 (2007), arXiv:hep-ex/0609009.

[16] D. V. Bugg, Reanalysis of data on $a_0(1450)$ and $a_0(980)$, Phys. Rev. D **78**, 074023 (2008), arXiv:0808.2706 [hep-ex].

[17] F. Ambrosino et al. (KLOE), Study of the $a_0(980)$ meson via the radiative decay $\phi \to \eta\pi^0\gamma$ with the KLOE detector, Phys. Lett. B **681**, 5 (2009), arXiv:0904.2539 [hep-ex].

[18] T. Aaltonen et al. (CDF), Measurement of branching ratio and B_s^0 lifetime in the decay $B_s^0 \to J/\psi f_0(980)$ at CDF, Phys. Rev. D **84**, 052012 (2011), arXiv:1106.3682 [hep-ex].

[19] G. S. Adams et al. (CLEO), Amplitude analyses of the decays $\chi_{c1} \to \eta\pi^+\pi^-$ and $\chi_{c1} \to \eta'\pi^+\pi^-$, Phys. Rev. D **84**, 112009 (2011), arXiv:1109.5843 [hep-ex].

[20] R. Aaij *et al.* (LHCb), Study of the lineshape of the $\chi_{c1}(3872)$ state, Phys. Rev. D **102**, 092005 (2020), arXiv:2005.13419 [hep-ex].

[21] V. Baru, J. Haidenbauer, C. Hanhart, A. E. Kudryavtsev, and U.-G. Meissner, Flatte-like distributions and the $a_0(980)/f_0(980)$ mesons, Eur. Phys. J. A **23**, 523 (2005), arXiv:nucl-th/0410099.

[22] A. Esposito, L. Maiani, A. Pilloni, A. D. Polosa, and V. Riquer, From the line shape of the $X(3872)$ to its structure, Phys. Rev. D **105**, L031503 (2022), arXiv:2108.11413 [hep-ph].

[23] R. Aaij *et al.* (LHCb), Study of the doubly charmed tetraquark T_{cc}^+, Nature Commun. **13**, 3351 (2022), arXiv:2109.01056 [hep-ex].

[24] V. Baru, X.-K. Dong, M.-L. Du, A. Filin, F.-K. Guo, C. Hanhart, A. Nefediev, J. Nieves, and Q. Wang, Effective range expansion for narrow near-threshold resonances, Phys. Lett. B **833**, 137290 (2022), arXiv:2110.07484 [hep-ph].

[25] A. M. Badalian, L. P. Kok, M. I. Polikarpov, and Y. A. Simonov, Resonances in Coupled Channels in Nuclear and Particle Physics, Phys. Rept. **82**, 31 (1982).

[26] K. Sone and T. Hyodo, Near-threshold hadron scattering with effective field theory, EPJ Web Conf. **291**, 05004 (2024), arXiv:2309.14631 [hep-ph].

[27] T. D. Cohen, B. A. Gelman, and U. van Kolck, An Effective field theory for coupled channel scattering, Phys. Lett. B **588**, 57 (2004), arXiv:nucl-th/0402054.

[28] E. Braaten, M. Kusunoki, and D. Zhang, Scattering Models for Ultracold Atoms, Annals Phys. **323**, 1770 (2008), arXiv:0709.0499 [cond-mat.other].

[29] X.-K. Dong, F.-K. Guo, and B.-S. Zou, Explaining the Many Threshold Structures in the Heavy-Quark Hadron Spectrum, Phys. Rev. Lett. **126**, 152001 (2021), arXiv:2011.14517 [hep-ph].

[30] T. Kinugawa and T. Hyodo, Compositeness of T_{cc} and $X(3872)$ by considering decay and coupled-channels effects, Phys. Rev. C **109**, 045205 (2024), arXiv:2303.07038 [hep-ph].

[31] L. Castillejo, R. H. Dalitz, and F. J. Dyson, Low's scattering equation for the charged and neutral scalar theories, Phys. Rev. **101**, 453 (1956).

[32] V. Baru, C. Hanhart, Y. S. Kalashnikova, A. E. Kudryavtsev, and A. V. Nefediev, Interplay of quark and meson degrees of freedom in a near-threshold resonance, Eur. Phys. J. A **44**, 93 (2010), arXiv:1001.0369 [hep-ph].

[33] Y. Kamiya and T. Hyodo, Structure of hadron resonances with a nearby zero of the amplitude, Phys. Rev. D **97**, 054019 (2018), arXiv:1711.04558 [hep-ph].

[34] T. Nishibuchi and T. Hyodo, Analysis of the $\Xi(1620)$ resonance and $\bar{K}\Lambda$ scattering length with a chiral unitary approach, Phys. Rev. C **109**, 015203 (2024), arXiv:2305.10753 [hep-ph].

[35] V. Baru, F.-K. Guo, C. Hanhart, and A. Nefediev, How does the $X(3872)$ show up in e^+e^- collisions: dip versus peak, (2024), arXiv:2404.12003 [hep-ph].